

ANL-6548

Incorporated by reference  
in 10 CFR

160

DO NOT DISCARD

1251

# Argonne National Laboratory

## STUDIES OF METAL-WATER REACTIONS AT HIGH TEMPERATURES

### III. EXPERIMENTAL AND THEORETICAL STUDIES OF THE ZIRCONIUM-WATER REACTION

by

Louis Baker, Jr. and Louis C. Just

### LEGAL NOTICE

*This report was prepared as an account of Government sponsored work. Neither the United States, nor the Commission, nor any person acting on behalf of the Commission:*

- A. Makes any warranty or representation, expressed or implied, with respect to the accuracy, completeness, or usefulness of the information contained in this report, or that the use of any information, apparatus, method, or process disclosed in this report may not infringe privately owned rights; or*
- B. Assumes any liabilities with respect to the use of, or for damages resulting from the use of any information, apparatus, method, or process disclosed in this report.*

*As used in the above, "person acting on behalf of the Commission" includes any employee or contractor of the Commission, or employee of such contractor, to the extent that such employee or contractor of the Commission, or employee of such contractor prepares, disseminates, or provides access to, any information pursuant to his employment or contract with the Commission, or his employment with such contractor.*

ARGONNE NATIONAL LABORATORY  
9700 South Cass Avenue  
Argonne, Illinois

STUDIES OF METAL-WATER REACTIONS AT HIGH TEMPERATURES  
III. EXPERIMENTAL AND THEORETICAL STUDIES  
OF THE ZIRCONIUM-WATER REACTION

by

Louis Baker, Jr.\* and Louis C. Just\*\*

May 1962

Preceding reports in this series:

- |          |                                                                                                                                                                                |
|----------|--------------------------------------------------------------------------------------------------------------------------------------------------------------------------------|
| ANL-6129 | Analog Computer Study of Metal-Water Reactions<br>Initiated by Nuclear Reactor Transients                                                                                      |
| ANL-6257 | Studies of Metal-Water Reactions at High Temper-<br>atures I. The Condenser Discharge Experiment:<br>Preliminary Results with Zirconium                                        |
| ANL-6250 | Studies of Metal-Water Reactions at High Temper-<br>atures II. TREAT Experiments: Status Report on<br>Results with Aluminum, Stainless Steel-304, Ura-<br>nium, and Zircaloy-2 |

\* Chemical Engineering Division

\*\* Applied Mathematics Division

Operated by The University of Chicago  
under  
Contract W-31-109-eng-38

## TABLE OF CONTENTS

	<u>Page</u>
I. ABSTRACT . . . . .	7
II. INTRODUCTION. . . . .	9
III. EXPERIMENTAL RESULTS. . . . .	13
A. Results of Runs in Room-temperature Water. . . . .	13
B. Results of Runs in Heated Water . . . . .	16
C. Results of Runs with Zircaloy-3 . . . . .	20
D. Metallurgical and X-ray Studies . . . . .	20
IV. MATHEMATICAL DESCRIPTION OF REACTION. . . . .	23
A. Calculation of Gaseous Diffusion Rates. . . . .	23
B. Calculation of Reaction Rate Controlled by Solid-state Processes . . . . .	27
C. Calculation of Heat Transfer Rates of Reacting Metal Spheres in Water . . . . .	28
D. Calculation of Temperature Drop Across the Oxide Film . . . . .	31
E. Summary of Equations. . . . .	31
V. RESULTS OF ANALOG COMPUTER STUDY . . . . .	33
A. Metal Property Values . . . . .	33
B. Trial-and-error Computation of the Rate Constant at 1852 C . . . . .	34
C. Comparison of Rate Constants with Those of Previous Investigators . . . . .	38
D. Calculation of Reaction in Heated Water . . . . .	38
1. Effect of Variations of the Emissivity and the Nusselt Number . . . . .	38
2. Effect of Initial Temperature and Particle Size . . .	
3. Temperature Drop Across the Oxide Film . . . . .	41
4. Comparison of Computed Extent of Reaction with Experimental Values. . . . .	42
5. Comparison of Computed Reaction Rates with Experimental Pressure Traces. . . . .	42
E. Calculation of Reaction in Room-temperature Water. . .	45
1. Effect of Water Vapor Pressure . . . . .	45
2. Comparison of Computed Extent of Reaction with Experimental Values. . . . .	48
3. Comparison of Computed Reaction Rates with Experimental Pressure Traces. . . . .	50

## TABLE OF CONTENTS

	<u>Page</u>
VI. DISCUSSION OF RESULTS AND COMPARISON WITH PREVIOUS STUDIES. . . . .	51
A. Reaction Scheme . . . . .	51
B. Total Extent of Reaction . . . . .	52
C. Conditions for Explosive Reaction. . . . .	53
D. Discussion of Parabolic Reaction . . . . .	54
E. Burning of Metal Vapor. . . . .	55
VII. APPLICATION TO REACTOR HAZARDS ANALYSIS. . . . .	58
A. Estimation of Zirconium-Water Reaction when Cladding Remains Intact . . . . .	58
B. Estimation of Zirconium-Water Reaction when Cladding is Melted . . . . .	59
1. Comparison with TREAT Studies. . . . .	60
2. Reactions with Uranium-Zirconium Alloys . . . . .	61
3. Effect of Water Temperature and Total Pressure. . . . .	62
VIII. REFERENCES. . . . .	64
IX. ACKNOWLEDGMENTS . . . . .	67
X. APPENDICES . . . . .	69
A. Experimental Data Tables . . . . .	69
B. Effect of Non-Planar Geometry on the Parabolic Rate Law . . . . .	74
C. Analog Computer Information. . . . .	77
D. Analysis of Rate Data Reported by Bostrom and Lemmon. . . . .	84

## LIST OF FIGURES

<u>No.</u>	<u>Title</u>	<u>Page</u>
1.	Zirconium Runs in Room Temperature Water . . . . .	14
2.	Pressure-Time Curves from Runs with 30-mil Zirconium Wires in Room Temperature Water . . . . .	15
3.	Zirconium-Water Reaction as a Function of Particle Diameter . . . . .	15
4.	Effect of Reaction Cell Free Volume and Added Inert Gas on the Zirconium-Water Reaction . . . . .	16
5.	Zirconium Runs in Heated Water. . . . .	17
6.	Pressure Traces from Runs with 60-mil Zirconium Wires in Heated Water. . . . .	18
7.	Pressure-Time Curves Taken from the Oscillograms of Figure 6. . . . .	18
8.	Effect of 20 psi Added Argon Gas on Reaction in Heated Water. . . . .	19
9.	Zirconium-Water Reaction as a Function of Particle Diameter . . . . .	19
10.	Runs with Zircaloy-3 . . . . .	20
11.	Photomicrographs of Oxidized Zirconium Particles from Condenser Discharge Runs. . . . .	21
12.	Hot Metal Sphere Reacting with Liquid Water . . . . .	24
13.	Variation of the Computed Extent of Reaction with Pre-exponential Factor . . . . .	34
14.	Computed Reaction and Temperature for two Values of Activation Energy. . . . .	35
15.	Computer Solution for Reactions of Zirconium Sphere with Water . . . . .	36
16.	Effect of Temperature on the Zirconium-Water Reaction. . .	37
17.	Computed Reaction and Temperature for 0.21-cm-diameter Zirconium Spheres in Heated Water. . . . .	39
18.	Computed Extents of Reaction and Temperatures for Molten Zirconium Spheres in Heated Water. . . . .	40
19.	Comparison of Computed and Experimental Results of Zirconium Runs in Heated Water. . . . .	42

## LIST OF FIGURES

<u>No.</u>	<u>Title</u>	<u>Page</u>
20.	Comparison of Experimental and Theoretical Pressure-Time Curves for Runs in Heated Water . . . . .	43
21.	Comparison of Experimental Results with Computed Results Based on Temperature Average Diffusion Rate for 60-mil Wires in Room Temperature Water . . . . .	47
22.	Computed Reaction and Temperature for 0.21-cm-diameter Zirconium Spheres in Room Temperature Water . . . . .	49
23.	Computed Reaction and Temperature for Molten Zirconium Spheres in Room Temperature Water. . . . .	49
24.	Comparison of Computed and Experimental Results of Zirconium Runs in Room Temperature Water . . . . .	49
25.	Comparison of Experimental and Theoretical Pressure-Time Curves for Runs in Room Temperature Water. . . . .	50
26.	Extent of Reaction as a Function of Particle diameter for Molten Zirconium Spheres Formed in Water. . . . .	52
27.	Graphical Representation of Parabolic Rate Law . . . . .	59

### Appendices

C-1	Symbols for Computer Elements . . . . .	81
C-2	Circuits for Solution of Equations . . . . .	82
C-3	Circuits for Solution of Equations . . . . .	83
C-4	Circuit for Control During Phase Change . . . . .	83
D-1	Reaction Between Zircaloy-2 and Steam. . . . .	85
D-2	Reaction Between Zircaloy-2 and Steam. . . . .	85
D-3	Reaction Between Zircaloy-2 and Water. . . . .	85
D-4	Reaction Between Zircaloy-2 and Water. . . . .	86

## LIST OF TABLES

<u>No.</u>	<u>Title</u>	<u>Page</u>
1.	Definition of Symbols . . . . .	26,27
2.	Definition of Constants Used in Computer Studies. . . . .	32
3.	Values of Constants Used in Computer Studies. . . . .	33
4.	Computed Results for Assumed Values of Activation Energy . . . . .	35
5.	Computed Results for the Reaction of Zirconium Spheres with Heated Water . . . . .	38
6.	Effect of Nusselt Number on the Reaction Rate for a Large Particle. . . . .	44
7.	Effect of Variations of $\Delta P_w/P$ on the Extent of Reaction of 0.21-cm Zirconium Spheres . . . . .	47
8.	Computed Results for the Reaction of Zirconium Spheres with Room Temperature Water . . . . .	48
9.	Zirconium-Water Reaction Studies . . . . .	53
10.	In-Pile Metal-Water Experiments in TREAT. . . . .	60
11.	Estimation of Relative Gaseous Diffusion Rates for Various Water Temperatures and Total Pressures. . . . .	63
<u>Appendices</u>		
A-1	Runs with 60-mil Zirconium Wires in Room Temperature Water. . . . .	70
A-2	Runs with 30-mil Zirconium Wires in Room Temperature Water. . . . .	71
A-3	Runs with 60-mil Zirconium Wires in Heated Water . . . . .	72
A-4	Runs with 60-mil Zircaloy-3 Wires . . . . .	73
D-1	Parabolic Rate Constants Recalculated from the Data of Bostrom and Lemmon. . . . .	86





# STUDIES OF METAL-WATER REACTIONS AT HIGH TEMPERATURES

## III. EXPERIMENTAL AND THEORETICAL STUDIES

### OF THE ZIRCONIUM-WATER REACTION

by

Louis Baker, Jr. and Louis C. Just

#### I. ABSTRACT

Further studies of the zirconium-water reaction by the condenser-discharge method are reported. The reaction was studied with initial metal temperatures from 1100 to 4000 C with 30- and 60-mil wires in water from room temperature to 315 C (1500-psi vapor pressure). Runs in heated water showed markedly greater reaction. This was explained in terms of a 2-step reaction scheme in which the reaction rate is initially controlled by the rate of gaseous diffusion of water vapor toward the hot metal particles and of hydrogen, generated by reaction, away from the particles. At a later time, the reaction becomes controlled by the parabolic rate law, resulting in rapid cooling of the particles.

A mathematical model of the reaction of molten metal spheres with water was proposed. The equations describing the reaction were programmed on an analog computer. The Nusselt number, describing both the gaseous diffusion rate and the rate of convection cooling, was given the theoretical minimum value for spheres, i.e.,  $Nu = 2$ , whereas the emissivity of the oxide surface was given the theoretical maximum value of unity. The only adjustable constants in the computer solutions were the parameters of the parabolic rate law. These were obtained empirically from the computer solutions and by reference to 2 previous isothermal studies of the zirconium-water reaction. The following rate law was deduced:

$$w^2 = 33.3 \times 10^6 t \exp(-45,500/RT)$$

where:  $w$  is milligrams of zirconium reacted per sq cm of surface area and  $t$  is time in sec.

Decreased extent of reaction in room-temperature water was best described on the assumption that in room-temperature water the effective vapor pressure of water, driving diffusion, is one-half the value in heated water. This was interpreted to mean physically that during reaction in room-temperature water the water surface facing heated particles is a dynamic mixture of water at the boiling point and water at room temperature.

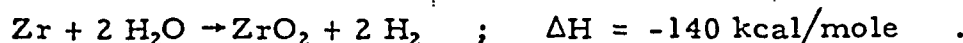
Explosive reactions were found to occur with particles smaller than about 1 mm in heated water and 0.5 mm in room-temperature water. The explosive reactions were due to the ability of the evolving hydrogen to propel the particles through water at high speed. The high-speed motion was detected on motion picture film and had the effect of removing the gaseous diffusion barrier (increasing the Nusselt number), resulting in very rapid reaction.

Computed results compared favorably with experimental results obtained by the condenser-discharge experiment and with the results of previous investigators. Computations indicated that the extent and rate of reaction depended on the particle diameter and the water temperature, and were relatively independent of the metal temperature so long as the metal was fully melted. This makes it possible to estimate the extent of zirconium-water reaction that would occur during a reactor accident in which the particle sizes of the residue could be estimated. Comparisons were made with the results of meltdown experiments in TREAT, and applications to reactor hazards analysis were discussed.



## II. INTRODUCTION

Chemical reactions between reactor cladding metals and water have been a subject of concern in the atomic energy program for many years. A coolant failure or a nuclear excursion in a water-cooled reactor would cause overheating of the fuel elements and might lead to a violent chemical reaction. The zirconium-water reaction is especially important because of the extensive use of zirconium and zirconium-based alloys as a fuel element cladding and structural material in water-cooled reactors. The following equation for the reaction shows that both heat and hydrogen gas are liberated by the reaction:



Chemical heat production could exceed the nuclear heat generation during a destructive nuclear transient.<sup>(1,2)</sup> Hydrogen generated by the reaction could give rise to a pressure surge and might subsequently react explosively with air. An investigation of the rates and mechanism of the zirconium-water reaction was therefore undertaken.

The literature of metal-water reaction studies was reviewed in 2 previous reports.<sup>(1,2)</sup> Previous results pertinent to the zirconium-water reaction will be summarized here. One of the first demonstrations that finely divided zirconium would react extensively with water was provided by Ruebsamen, Shon, and Chrisney.<sup>(3)</sup> They employed condenser-discharge heating to melt rapidly 2-mil foil strips of zirconium under water. They determined the extent of reaction by collecting hydrogen generated by reaction in the absence of air. The extent of reaction ranged between 20 and 100 percent for 5 runs with zirconium.

Bostrom studied the isothermal oxidation rates of Zircaloy-2 cylinders by induction heating under water.<sup>(4)</sup> Continuous measurements of the hydrogen evolution were made at metal temperatures between 1300 and 1860 C. The results could be described approximately by a parabolic rate law. Oxidation was very similar to the air oxidation of zirconium. Rates were rapid but not explosive at temperatures up to and slightly above the melting point.

Lustman used Bostrom's data to make quantitative predictions of the results of a loss-of-coolant accident in PWR.<sup>(5)</sup> Lustman was able to estimate the heating curve of Zircaloy-2 in the core structure due to the heat released in the chemical reaction and the residual fission product decay. He also determined the cooling curve of a molten droplet in water, considering thermal radiation as the only cooling mechanism. The results were very sensitive to the assumed emissivity value.

Milich and King melted zirconium rod and dropped 10-20 gram batches into water under various conditions of temperature and pressure.<sup>(6)</sup> They used induction heating within a high-pressure autoclave. They found that high pressures of inert gas suppressed the reaction whereas high steam pressure gave very extensive reaction.

Lorentz used static irradiation in MTR to simulate a "run-away" reaction incident using zirconium-uranium alloys.<sup>(7)</sup> Alloy samples were loaded into high-pressure autoclaves and lowered into the MTR core for periods of about 15 sec. Heating rate was estimated from the flux and the sample enrichment to be about 5000 F/sec. From 16 to 84 percent of the alloy reacted, as determined by the volumes of hydrogen collected from the autoclaves in 5 different runs.

Elgert and Brown conducted a similar study in MTR using fuel plates clad with zirconium.<sup>(8)</sup> Results were very similar to those reported by Lorentz, in that very extensive reaction of the zirconium occurred. Sporadic explosions were recorded during the irradiation in some cases.

Layman and Mars<sup>(9)</sup> demonstrated a self-sustaining reaction between Zircaloy and water, by condenser-discharge heating to simulate exponential periods of 2 to 20 msec. Chemical reaction was initiated very close to the melting point. Some self-heating was noted in every run, and reaction in some runs was sustained to completion.

Extensive studies of metal-water reactions were reported by Higgins et al. of the Aerojet General Corporation.<sup>(10-12)</sup> One-inch-diameter streams of molten zirconium were discharged into water in one study. Only a thin oxide coating was formed on the resulting metal globules. In some experiments, blasting caps were used to obtain dispersion of the molten metal; the metal was converted largely into spherical particles. This procedure resulted in violent reactions of water with zirconium, Zircaloy-2, and Zircaloy-B. It was determined that the percent reaction was a sensitive function of particle size. Finer particles gave much more reaction. Studies with an alloy of Zircaloy-B and 0.9% beryllium gave somewhat less reaction. Reaction could be approximated by assuming that all particles were oxide coated to a thickness of 25  $\mu$ .

In another study, 10-20 g of molten zirconium were sprayed under pressure into water in the Aerojet Explosion Dynamometer.<sup>(12)</sup> Spherical particles were formed as in the previous study, and the extent of reaction was determined as a function of particle size by measurement of the thickness of oxide layer. The transient pressures generated within the water column were used to calculate the work, total impulse, and mechanical efficiency of the explosion. Results indicated that reactions became more violent when the initial metal temperature was greater than 2400 C.

Saltsburg<sup>(13)</sup> reviewed previous experimental studies of metal-water reactions in an attempt to relate them to nuclear incidents. Both the loss-of-coolant and the nuclear-runaway incidents were discussed. The importance of external hydrodynamical and heat transfer considerations was stressed. It was pointed out that the nature of the reaction becomes governed by physical processes rather than by chemical processes at some high temperature which is probably well below the vaporization point of the metal.

A series of studies relating to the zirconium-water reaction were reported by Lemmon *et al.* of the Battelle Memorial Institute.<sup>(14)</sup> Determinations of the total and spectral emissivities of Zircaloy and zirconium dioxide were reported as a part of this program. A study was also made of the diffusion of oxygen into solid Zircaloy at high temperatures. Another phase of the program involved a study of the reaction between solid Zircaloy-2 and steam between 1000 and 1690 C. After unreacted steam was condensed, the reaction rate was determined by measuring the quantity of hydrogen produced. The results were best correlated in terms of the parabolic rate law with an activation energy of 34 kcal per mole. They also calculated an activation energy of 65.4 kcal per mole for Bostrom's data.<sup>(4)</sup> Steam pressure had little or no effect on the reaction rate. In another study, molten Zircaloy globules were formed by induction heating the end of a rod. The globules were dropped into water. The thickness of oxide layer was measured as a function of water temperature. Uncertainty about whether the globules were fully melted or not apparently caused considerable scatter in the data. Cooling time increased markedly with increasing water temperature. A final study reported by Battelle<sup>(14)</sup> was a mathematical analysis to determine the amount of reaction and heat transfer that would occur for a molten Zircaloy droplet falling through a steam and water environment. Bostrom's data were used for the analysis. The analysis considered the fact that convection heat transfer at the leading edge of a falling drop is greater than that at the trailing edge. This led to the difficulty that in some cases the temperature at each end of the droplet diverged. It also led to the conclusion that larger drops react more extensively than smaller drops, which was inconsistent with most experimental results.

A series of studies of metal-water reactions were carried out by General Electric Company under the direction of L. F. Epstein.<sup>(15-23)</sup> Six reports<sup>(15-18,21,22)</sup> presented analyses of reactor behavior which might set the stage for destructive metal-water reactions. Another report discussed analytical formulations of rate laws which might be applicable to metal-water reactions.<sup>(20)</sup> Zirconium was exposed to water vapor contained in an inert carrier gas in one study.<sup>(19)</sup> It was determined that the reaction rate of clean surfaces of solid zirconium was controlled by the rate of gaseous diffusion of water vapor through the carrier gas. A demonstration of the levitation melting technique as applied to zirconium

was reported in another study.<sup>(23)</sup> A rapid-recording infrared pyrometer was used to follow temperature changes produced by reaction.

A more recent paper by Epstein pointed out the coincidence of the reported ignition temperatures of several metals with the temperature where the metal vapor pressure reaches 0.15 mm.<sup>(24)</sup> This was taken to indicate that metal-water reactions become violent because of a vapor-phase initiating reaction.

The foregoing discussion of the literature showed that the zirconium-water reaction is relatively slow and corrosion-like under most conditions, especially when large pieces of metal are involved. Several investigators reported explosions, self-sustained burning, or very extensive reaction when finely divided metal was involved.

The previous studies did not provide a quantitative understanding of what particle sizes and/or metal temperature leads to an explosive reaction. The results of 2 studies of the isothermal oxidation rates of Zircaloy at temperatures below the melting point did not agree with each other. No satisfactory rate measurements have been reported for the molten metal. Previous papers have discussed many physical and chemical processes which may be involved in the overall reaction, i.e., gaseous diffusion, solid-state diffusion, adsorption, metal vaporization, convection, radiation, boiling heat transfer, etc. It is not clear, however, which process or processes control the reaction rate.

Studies of the zirconium-water reaction were therefore undertaken in the Chemical Engineering Division of Argonne National Laboratory. These studies used the condenser-discharge method to investigate the reaction at high temperatures. A preliminary report<sup>(1)</sup> described the selection of the condenser-discharge method and the experimental procedures in detail. Some experimental results were also reported.

This paper gives further experimental results obtained by the condenser-discharge experiments and describes a mathematical model of the reaction which is compared to the experimental results of this and previous studies of the reaction. Some preliminary conclusions pertaining to reactor hazards analyses are also presented.

### III. EXPERIMENTAL RESULTS

The experimental studies were carried out by the condenser-discharge method.\* The maximum energy that could be stored in the condensers was 296 cal, which could be delivered to a circuit consisting of a one-inch-long specimen wire, either 30 or 60 mils in diameter, and extraneous lead resistance in a nominal time of 0.3 msec (0.0003 sec). The energy actually received by the specimen wire could be determined accurately by electrical measuring methods. The energy per gram of specimen wire was used with enthalpy data to calculate the initial metal temperature on the assumption that uniform adiabatic heating had occurred. High-speed motion pictures and the correspondence between calculated initial temperatures and indications of melting verified the assumption.

Specimen wires were immersed in degassed water in one of 2 stainless steel reaction cells. One reaction cell was used with water at room temperature (low-pressure cell), and the other was used with water from room temperature to 315 C (vapor pressure of 1500 psi). The low-pressure cell contained Pyrex windows through which high-speed motion pictures were taken.

Piezoelectric pressure transducers were mounted on both reaction cells. A recording of transient pressure for each run was obtained by photographing the screen of a cathode-ray oscilloscope. The pressure traces were affected by the discharge current during the first few msec of most runs, making it impossible to measure peak explosion pressures.

The hydrogen generated by reaction was collected and the quantity determined. From this and the specimen weight, the percent of metal reacted in each run was determined. Residue from runs was collected and average particle size determined. Residue was examined metallographically and by X-ray diffraction techniques.

#### A. Results of Runs in Room-temperature Water

The data for all condenser-discharge runs are presented in tables in Appendix A. The results of hydrogen analyses expressed as percent of metal reacted are plotted in Figure 1 as a function of the initial metal temperature for zirconium runs in room-temperature water. The atmosphere above the water in the reaction cell in these runs was air-free; the initial pressure was therefore the vapor pressure of water at room temperature (ca. 0.5 psia). The results show that the percentage of metal that reacted in nominal 30-mil wire specimens was approximately twice that in

---

\*The reader is referred to Ref. 1 for a more detailed description of the experimental procedures.



nominal 60-mil wire for runs at metal temperatures up to and including the melting point region. The results also show that at an initial metal temperature of 2600 C there was a sharp transition from a maximum of 20 percent reaction to as much as 70 percent reaction.

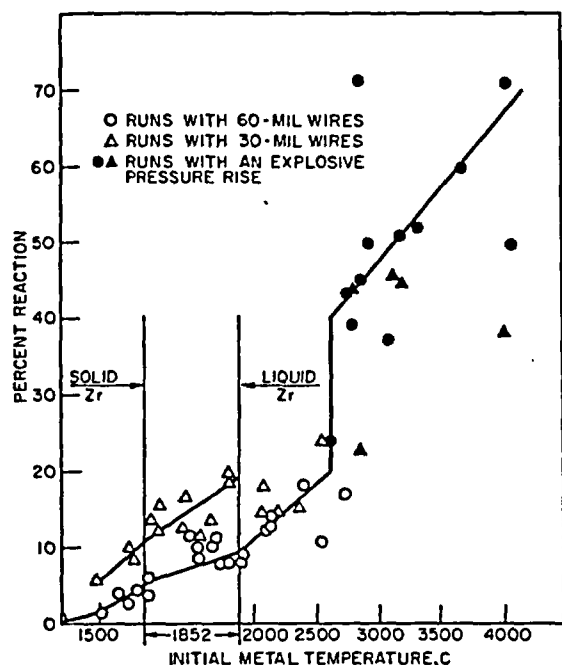


Figure 1  
ZIRCONIUM RUNS IN ROOM  
TEMPERATURE WATER  
(See Tables A1 - Part I and A2  
for tabular data)

There was a sharp change in the character of the transient pressure traces at initial metal temperatures of the order of 2600 C. Pressure-time curves from typical runs (previously presented in Figure 18 of ANL-6257) are reproduced in Figure 2. Runs with initial metal temperatures less than 2600 C had slow rates of pressure rise as shown in curves a, b, c, and d of Figure 2. Several tenths of a second were required for the pressure to approach a final value. Runs with initial metal temperatures exceeding ca. 2600 C had an explosive pressure rise, as shown in curves e and f of Figure 2; a final pressure was reached within a few milliseconds.

The results shown in Figure 1 imply that initial metal temperature is the principal variable which determines the extent of reaction. Particle size has been shown by previous investigators to be of major importance. The results are therefore plotted as a function of mean particle diameters\* in Figure 3 without considering the initial metal temperature. Plotted in this way, there is little difference between runs made with 30- and 60-mil wires. There is also no sharp break in the curve between explosive and nonexplosive runs. The ignition might be considered as a critical particle size phenomenon as well as a critical temperature phenomenon, since nonexplosive runs had mean particle diameters in excess of 650  $\mu$ , whereas all but one explosive run had mean particle diameters below 500  $\mu$ .

\*The Sauter mean diameter was used to represent the particle size.

Figure 2

PRESSURE-TIME CURVES FROM RUNS  
WITH 30-MIL ZIRCONIUM WIRES IN  
ROOM-TEMPERATURE WATER

Run No.	Initial Metal Temp, C, and Physical State	Final Pressure Rise, atm
(a) 86	1700, Solid	0.11
(b) 82	1852, 100% Liquid	0.16
(c) 106	2100, Liquid	0.16
(d) 74	2500, Liquid	0.22
(e) 109	2800, Liquid	0.44
(f) 114	(482 cal/g) Vapor	0.46

(Pressure Traces Shown in Ref. 1)

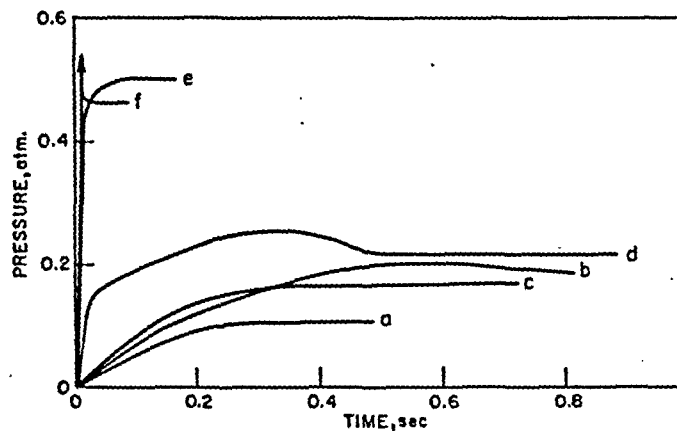
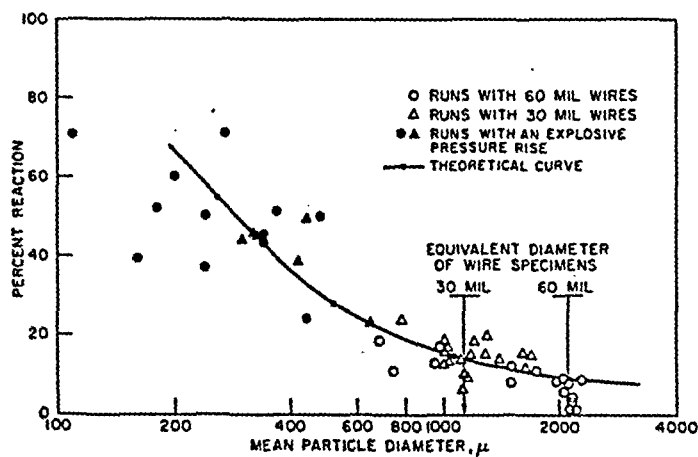


Figure 3

EFFECT OF PARTICLE DIAMETER ON  
ZIRCONIUM-WATER-REACTION IN  
ROOM TEMPERATURE WATER

(See Tables A1 - Part I and A2  
for tabular data)



Three series of runs with nominal 60-mil wires were made, one series with an atmosphere of inert gas above the water in the reaction cell. It was recognized, however, that a run without added inert gas generates hydrogen, which presumably acts as inert gas pressure above the water level. An attempt was therefore made in another series of runs to reduce the average inert gas pressure. This was done by enlarging the gas volume of the reaction cell from a normal value of 40 cc to about 160 cc. The results of a series of runs with 60-mil wires in the large-volume cell are compared with normal runs and inert gas runs in Figure 4. The results show that, on the average, there was a slightly increased reaction in the large-volume cell. There was no significant decrease in reaction, however, in the presence of 1 atm of added inert gas.

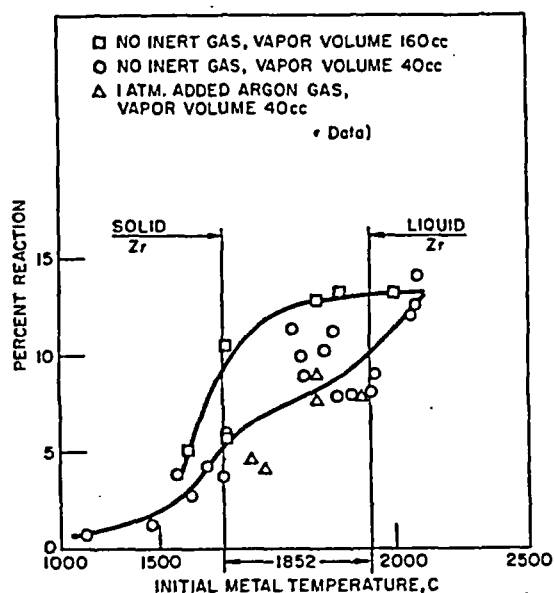


Figure 4

#### EFFECT OF REACTION CELL FREE VOLUME AND ADDED INERT GAS ON THE ZIRCONIUM-WATER REACTION

(60-mil wires; room-temperature water)

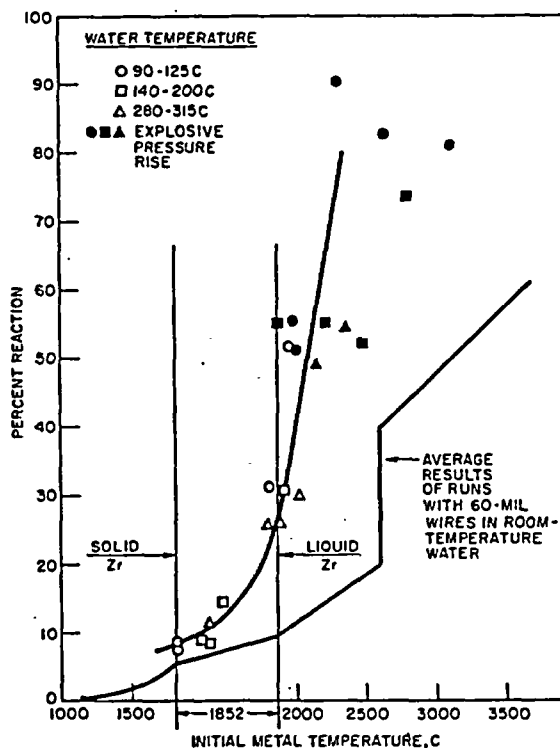
(See Table A1 for tabular data)

#### B. Results of Runs in Heated Water

Several series of runs were made in the high-pressure reaction cell with heated and degassed water in the absence of air or other inert gas. Water temperature was varied from 90 C (vapor pressure of 10 psia) to 315 C (vapor pressure of 1500 psia). The results of runs in heated water are shown in Figure 5. The average line for runs with 60-mil wires in room-temperature water was taken from Figure 1 and included on Figure 5 for comparison. Reaction in heated water was much more extensive than in room-temperature water. The extent of reaction, however, did not increase uniformly with water temperature or vapor pressure. Reaction was identical in runs with nominal 100 C water and runs made with 315 C water, even though the pressures were 10 psi and 1500 psi in these runs.

Figure 5  
ZIRCONIUM RUNS IN HEATED WATER  
(60-mil wires)

(See Table A3, Sections I, II, and III,  
for tabular data)



Runs in heated water could be divided into explosive and nonexplosive runs in the same manner as runs in room-temperature water. The apparent ignition temperature was ca. 1900 C. The transition from runs with a slow pressure rise to runs with an explosive pressure rise was not, however, as sharply defined as it was with room-temperature runs. Pressure-time traces were obtained which appeared to be composites of both slow and explosive rates. Transient pressure traces reproduced from the oscilloscope camera are shown in Figure 6. The traces are ordered according to the initial metal temperature; the steam pressure had no effect on the character of the pressure traces over the range from 19 to 1500 psia. Pressure-time plots deduced from the traces are given in Figure 7. Trace b shown in Figures 6 and 7 appears to represent the condition in which about one-half of the reaction results from particles reacting explosively (in a few msec) and one-half from particles reacting slowly (one-tenth to several tenths of a second). Trace a of Figures 6 and 7 indicates that the entire metal sample had the slow pressure rise. The d and e traces of Figures 6 and 7 indicate that the entire sample reacted explosively.

Figure 6

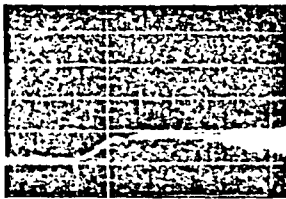
PRESSURE TRACES FROM RUNS WITH 60-MIL  
ZIRCONIUM WIRES IN HEATED WATER

Run No.	Initial Metal Temp, C, and Physical State	Initial Steam Pressure, psia	Final Pressure Rise, atm <sup>a</sup>	Vertical Sensitivity, atm/cm <sup>b</sup>	Horizontal Sweep Rate, sec/cm <sup>b, c</sup>
(a) 191	1852, Solid	32	0.42	1.35	0.20
(b) 234	1852, 90% Liquid	1500	3.0	4.75	0.20
(c) 230	2100, Liquid	1500	4.8	11.9	0.20
(d) 217	2300, Liquid	19	6.1	3.33	0.20
(e) 220	2800, Liquid	150	5.7	9.50	0.20

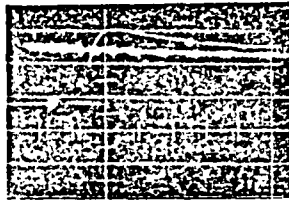
<sup>a</sup>Intense return trace gives final pressure rise.

<sup>b</sup>Major grid divisions are 1 cm apart on the scope face.

<sup>c</sup>Beam is interrupted once each second.



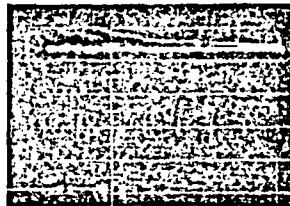
a



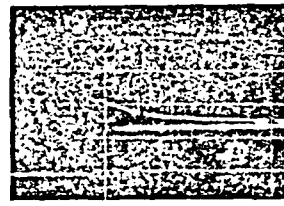
b



c



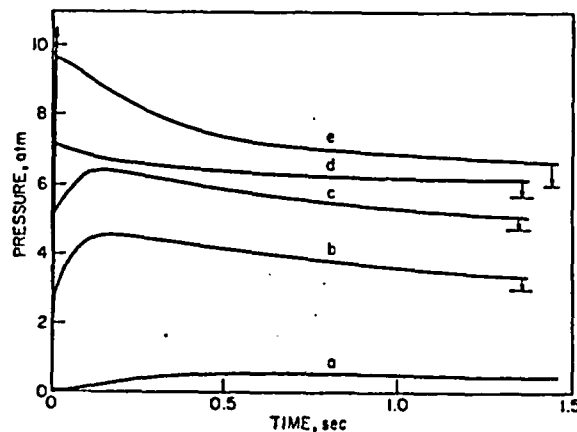
d



e

Figure 7

PRESSURE-TIME CURVES TAKEN  
FROM THE OSCILLOGRAMS  
OF FIGURE 6



Several runs were made to test the effect of added inert gas on the reaction of zirconium in heated water. Water temperature was about 110 C (vapor pressure of 20 psi), and 20 psi of argon was added to the reaction cell in these runs. The runs are compared in Figure 8 with the average line (see Figure 5) obtained from all of the heated water runs. The results indicated that there was no significant effect of 20 psi inert gas.

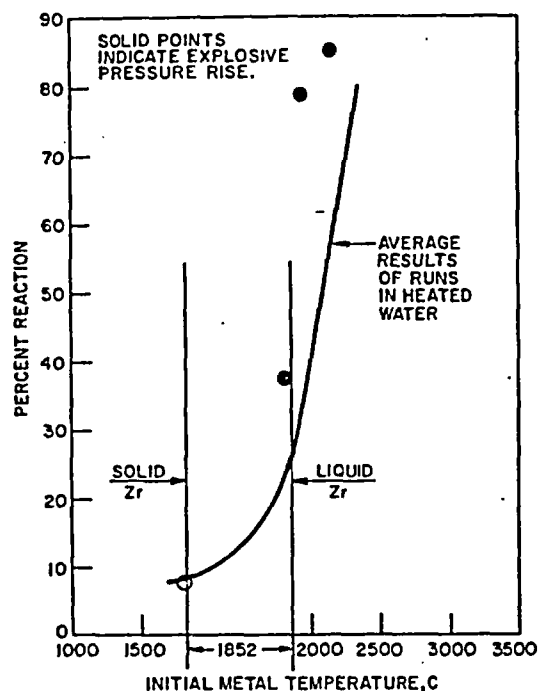
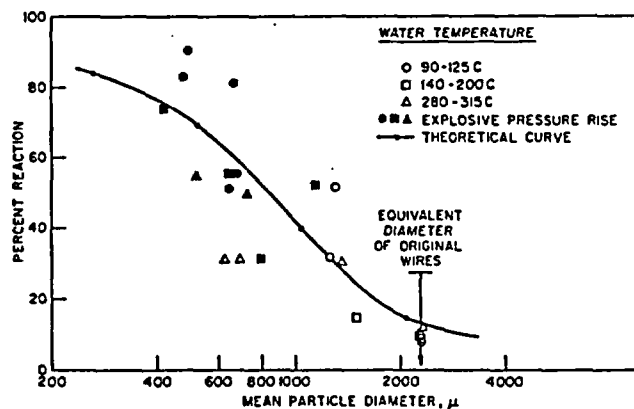


Figure 8  
EFFECT OF 20 PSI ADDED ARGON  
GAS ON REACTION IN  
HEATED WATER  
(See Table A3, Part IV, for  
tabular data)

Results of runs in heated water are plotted as a function of particle size in Figure 9. More scatter is apparent than in runs in room-temperature water (compare with Figure 3). The results are similar to those in room-temperature water in that there is no definite break between explosive and nonexplosive runs.

Figure 9  
ZIRCONIUM-WATER REACTION AS A  
FUNCTION OF PARTICLE DIAMETER  
(Heated water; 60-mil wires)  
(See Table A3, Sections I, II, and III for tabular data)



### C. Results of Runs with Zircaloy-3\*

A series of runs with Zircaloy-3 wires (of nominal 60-mil diameter) were made in room-temperature water and in heated water. The results are plotted in Figure 10. The average line for runs with 60-mil zirconium wires is included on the figure for comparison. The results show that when the condenser-discharge method is used, there is no detectable difference in percent reaction between pure zirconium and Zircaloy-3.

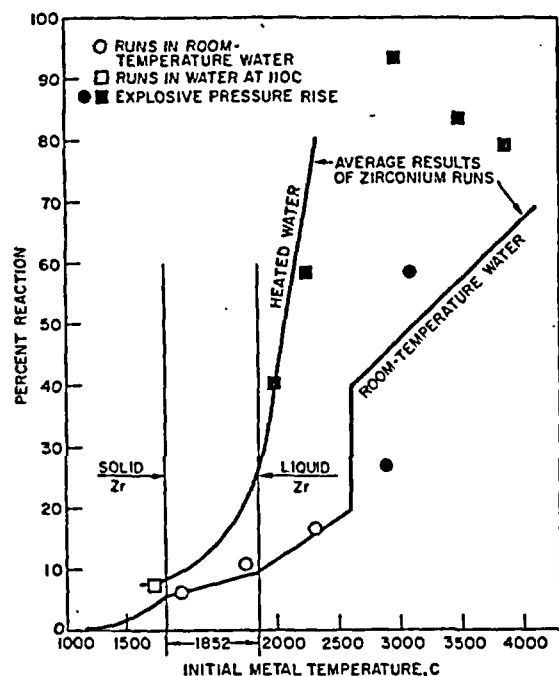


Figure 10

RUNS WITH ZIRCALOY-3  
(See Table A4 for tabular data)

### D. Metallurgical and X-Ray Studies

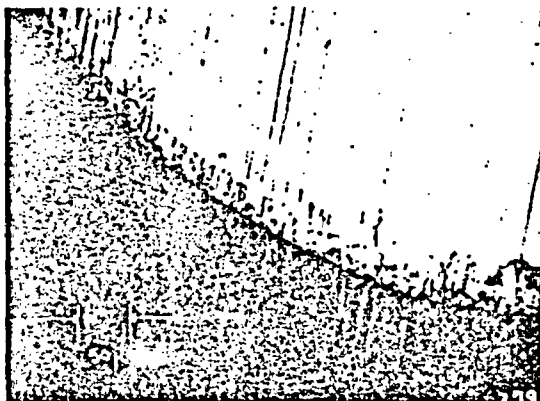
A series of photomicrographs were taken of typical particles obtained from the residue of condenser-discharge runs. These are shown in Figure 11.\*\* Microscopic studies showed that most particles were very nearly spherical and that most particles had very uniform oxide films. In some cases, a circular zone was apparent between the outer oxide film and the interior of the particle. This was reported by Lemmon<sup>(14)</sup> to be an alpha-solid-solution phase consisting of alpha-zirconium containing dissolved oxygen. The metal in the interior of the particles was also alpha-zirconium; however, it had the somewhat different appearance that is characteristic of metal which has been transformed from the beta-phase during cooling.

\*Zircaloy-3 is a zirconium alloy containing 0.2 to 0.3 weight percent each of tin and iron with trace quantities of other elements.

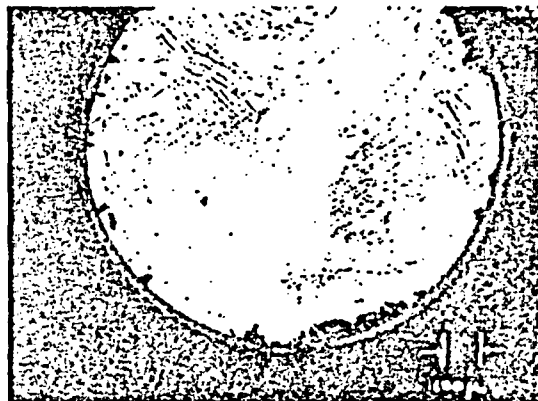
\*\*The specimens were mounted in plastic and ground to a 600 grit finish. They were neither polished nor etched.

Figure 11

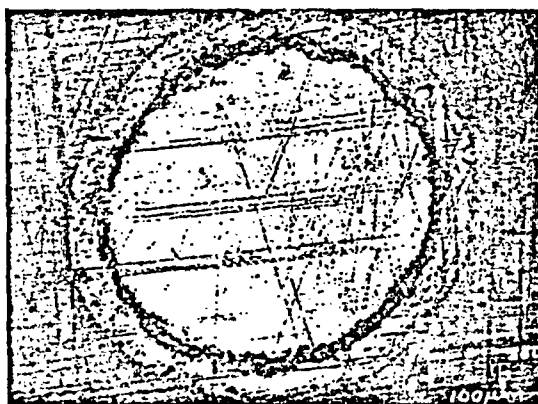
PHOTOMICROGRAPHS OF OXIDIZED ZIRCONIUM PARTICLES  
FROM CONDENSER-DISCHARGE RUNS



a. Initial Metal Temp: 1800 C; Room-temp Water (run 22, cross section of cylinder).



b. Initial Metal Temp: 1852 C; 100% melted; Room-temp Water (run 90).



c. Initial Metal Temp: 1852 C; 100% melted; Heated Water (run 200).



d. Initial Metal Temp: 1900 C; Room-temp Water (run 15).



e. Initial Metal Temp: 2400 C; Room-temp Water (run 305).



f. Initial Metal Temp: 2900 C; Room-temp Water (run 302).



Some of the smaller particles that had reached very high temperatures had an irregular appearance, which suggested that oxide had broken off during cooling or, in some cases, during procedures for metallurgical preparation. Unreacted metal containing large amounts of dissolved oxygen is known to be very brittle, which would account for the difference in strength for lightly oxidized and heavily oxidized particles.

Particles obtained from runs in room-temperature water were uniformly black in appearance, which suggested that no particles were completely oxidized. Many of the smaller particles from runs in heated water were pure white, resembling small pearls, which suggested that they were completely reacted. These particles generally could not be mounted in Lucite and ground without damage.

X-ray diffraction studies were made of particles from runs in room-temperature and heated water and over a wide range of initial metal temperatures. The only phases found to be present in the residue were alpha-zirconium and monoclinic zirconium dioxide. The white particles showed only monoclinic zirconium dioxide.

Analyses for the quantity of hydrogen retained by the oxidized specimens were made in the Battelle studies.<sup>(14)</sup> It was found that in runs at 1000 to 1600 C, between 4 and 13 percent of the hydrogen formed in the reaction of steam with Zircaloy-2 is absorbed in the sample. Less than one percent of the hydrogen was retained in runs at temperatures between 1900 and 2050 C. The Battelle results suggested that a negligible amount of hydrogen was retained in runs with fully melted metal. These results were the basis for the assumption that the quantity of hydrogen gas collected is an accurate measure of the quantity of metal reacted.

#### IV. MATHEMATICAL DESCRIPTION OF REACTION

Several attempts to compute the temperature-time and reaction-time history of a hot zirconium droplet in water have been made by previous investigators.<sup>(5,14)</sup> These investigators used the isothermal data of Bostrom<sup>(4)</sup> and were required to extrapolate these data to higher temperatures. Bostrom's data and the later data by Lemmon<sup>(14)</sup> indicated a large temperature coefficient of reaction rate (and thus a high activation energy). Reaction rates extrapolated from data involving a high activation energy become very fast, especially when very little oxide has built up on the metal.

Experimental results presented in the previous chapter, however, provide several indications that a reaction rate that increases rapidly with temperature is not realized experimentally. The results in Figure 1 show that very little increased reaction occurs when the initial metal temperature is increased from 1852 to 2600 C in room-temperature water.

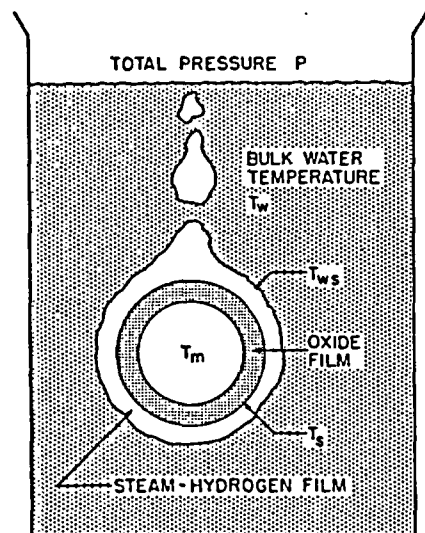
It thus became important to consider what processes other than diffusion through the oxide film, essential to a heterogeneous reaction, might be slow and hence rate-controlling at high temperatures. Several authors have pointed out that a process of gaseous diffusion is also involved in the reaction of metal drops with water or steam.<sup>(13,22)</sup> It is necessary for water vapor to diffuse to the surface of a partly oxidized globule and for the hydrogen generated by the metal-water reaction to diffuse away from the globule. If the rate of this process is slower than rates indicated by extrapolation of isothermal rate data, then clearly the reaction will not proceed at the high extrapolated rates. The increased reaction occurring in heated water also suggests that gaseous diffusion may play a role. Gaseous diffusion would depend on the vapor pressure of the water. When this is very low (0.5 psi for room-temperature water), the reaction might be seriously impeded.

A study of the literature of gaseous diffusion was, therefore, undertaken to determine how diffusion rates could be formulated and included into a calculation scheme similar to those of previous investigators.<sup>(5,14)</sup>

##### A. Calculation of Gaseous Diffusion Rates

A reacting metal droplet in a water environment is sketched in Figure 12. The droplet is completely surrounded by a gaseous film of steam and hydrogen. One author has suggested that a direct reaction between metal and liquid water is responsible for rapid reactions.<sup>(3)</sup> A very thorough discussion of the amount of superheat that can be accepted by a liquid was given by Westwater as part of a review of boiling processes.<sup>(25)</sup> Both an argument based on thermodynamics and one based on the kinetics of bubble nucleation indicate that a liquid cannot exist, even

Figure 12  
HOT METAL SPHERE  
REACTING WITH LIQUID  
WATER



instantaneously, above a certain temperature. There would then be a critical temperature difference between a hot solid and a liquid beyond which liquid could not exist in direct contact with the surface of the solid. Unfortunately, it is not possible to state an exact value for this limiting temperature for a particular case. For water at one atmosphere, the limiting surface temperature is between the boiling point (100 C) and the critical point (374 C) of water. These temperatures are far below the range of interest in metal-water studies. It is reasonable, therefore, to assume that there is always a complete vapor film surrounding the metal droplet.

It is important to determine whether the process of gaseous diffusion can be considered as a steady-state process with a constant vapor film thickness or whether it must be treated as a transient process with a continually enlarging

film. It is also important to determine how much reaction occurs before a diffusion barrier is established. At the instant of creation of the metal droplet, there is no hydrogen in the gaseous film and there is, therefore, no diffusion barrier. Initial reaction will be very rapid. It is of interest to compute how much reaction is required to produce enough hydrogen to form a bubble of radius  $2x_0$ , where  $x_0$  is the radius of the metal sphere, since a film thickness of  $x_0$  approaches the size required for a minimum rate of gaseous diffusion.

The volume ratio of 2 moles of hydrogen\* to that of one gram-atom of zirconium is 3500. Thus 0.2% reaction would result in 7 times as much gas volume as metal volume, which would produce a bubble having twice the radius of the metal droplet. In reality, the bubble would be much larger because the average hydrogen temperature would be much higher than room temperature. There would be steam in the bubble as well as hydrogen. It is apparent that a very slight reaction would produce a sizable film if the entire quantity of hydrogen were retained in the bubble. As more and more reaction occurred, it is likely that bubbles would leave the film more or less regularly, resulting in a more or less constant film thickness. Both diffusion and heat transfer across the film might then be considered as steady-state processes.

A previous author has stressed the importance of the initial reaction, i.e., the reaction of clean metal.<sup>(19)</sup> It seems clear that the initial reaction rate will exceed the steady-state rate. On the other hand, the

\*Hydrogen is assumed to be at 1 atm and room temperature.

rapid initial reaction should subside after less than 0.2% of the metal has reacted because of the thickness of the hydrogen film. If the initial 0.2% reaction occurred adiabatically, the metal temperature would rise only 35 C.\* The temperature rise, the extent of reaction, and the quantity of hydrogen produced before gaseous diffusion can come into play would be rather minor. These quantities, moreover, are independent of particle size.

The rate of steady-state diffusion of water vapor through a spherical steam-hydrogen film can be formulated as a mass transfer coefficient  $h_d$  times the area of a sphere,  $4\pi x_0^2$ , times the difference in concentration of water vapor across the film,  $\Delta P_w/RT_f$ , as follows<sup>(26)</sup> (symbols are defined in Table 1):

$$\text{moles H}_2\text{O/sec} = h_d(4\pi x_0^2)(\Delta P_w/RT_f) \quad (1)$$

The mass transfer coefficient can be expressed in the Nusselt form:

$$\text{Nu} = h_d 2x_0/D \quad (2)$$

and the mean film temperature can be taken as an average between the metal surface temperature and the bulk water temperature:

$$T_f = \frac{1}{2} (T_s + T_w) \quad (3)$$

Values of the diffusion coefficient  $D$  for the hydrogen-water system were calculated by Furman.<sup>(19)</sup> His results can be represented approximately as follows:

$$D = D_0 T_f^{1.68}/P \quad (4)$$

where  $D_0 = 6.52 \times 10^{-5} \text{ (sq cm)(atm)/(sec) (K}^{1.68}\text{)}$ . Substituting Equations 2, 3, and 4 into Equation 1 yields

$$\text{moles H}_2\text{O/sec} = \text{Nu} \frac{D_0 2\pi x_0}{R 2^{0.68}} (T_s + T_w)^{0.68} \frac{\Delta P_w}{P} \quad (5)$$

For purposes of calculation, it was most convenient to express the diffusion rate as the linear rate at which the oxide film advances into unreacted metal when reaction is controlled by gaseous diffusion:

$$\text{moles H}_2\text{O/sec} = \frac{-\rho_m n}{M_m} (4\pi x^2) \left( \frac{dx}{dt} \right)_{\text{diffusion}} \quad (6)$$

---

\*Temperature rise is ca. 0.002 times the heat of reaction divided by the specific heat of metal or  $(0.002)(140,000 \text{ cal/gm-atom})/(8.0 \text{ cal/g-atom/deg C})$ .

The diffusion-controlled reaction rate is then obtained by combining Equations 5 and 6 as follows:

$$-\left(\frac{dx}{dt}\right)_{\text{diffusion}} = \frac{\text{Nu} D_0 M_m}{2^{1.68} \rho_m n R} \frac{x_0}{x^2} (T_s + T_w)^{0.68} \frac{\Delta P_w}{P} \quad (7)$$

Table 1

DEFINITION OF SYMBOLS

A	is pre-exponential factor in parabolic rate law, $\text{mg}^2/(\text{cm}^4)(\text{sec})$
$C_p$	is specific heat, $\text{cal}/(\text{mole})(\text{K})$ or $\text{cal}/(\text{g})(\text{K})$
D	is diffusion coefficient, $\text{sq cm}/\text{sec}$
$\Delta E$	is activation energy, $\text{kcal}/\text{mole}$
$\epsilon$	is total emissivity of oxide surface
F	is fraction of original metal in liquid state
H	is heating rate, $\text{cal}/\text{sec}$
h	is heat transfer coefficient, $\text{cal}/(\text{sec})(\text{sq cm})(\text{K})$
$h_d$	is mass transfer coefficient, $\text{cm}/\text{sec}$
k	is thermal conductivity, $\text{cal}/(\text{sec})(\text{cm})(\text{K})$
L	is heat of fusion, $\text{cal}/\text{mole}$
M	is molecular weight, $\text{g}/\text{mole}$
n	is moles of hydrogen generated per atom of metal reacted
Nu	is Nusselt number
$\Delta P_w$	is partial pressure of water vapor driving diffusion, atm
P	is total pressure, atm
Q	is heat of reaction, $\text{cal}/\text{mole}$
R	is gas constant, $(\text{cc})(\text{atm})/(\text{mole})(\text{K})$ or $(\text{cal})/(\text{mole})(\text{K})$
$\rho$	is density, $\text{g}/\text{cc}$ or $\text{moles}/\text{cc}$
$\sigma$	is Stefan Boltzmann constant, $\text{cal}/(\text{sec})(\text{sq cm})(\text{K}^4)$
t	is time, sec
T	is temperature, K
x	is radius of unreacted metal, liquid or solid, cm
$x_0$	is original radius of unreacted metal, cm

Table 1 (Cont'd.)

Subscripts:

f	refers to the diffusion film
m	refers to the metal
ox	refers to the oxide
s	refers to the oxide surface
w	refers to the bulk of the water

The principal unknown factor in Equation 7 is the Nusselt number, Nu. Fortunately, there is a theoretical minimum Nusselt number,  $Nu = 2$ , for diffusion or heat transfer to a sphere.<sup>(27)</sup> This occurs physically because, as the gaseous film increases in size and the diffusion path becomes longer, the spherical area normal to diffusion increases greatly. The greater area overrides the longer diffusion path and a minimum Nusselt number obtains regardless of how large the diffusion film becomes. If the particle is in violent motion, however, the mean film thickness can become very small and the Nusselt number can become greater than 2. The theoretical minimum value of 2 is approached accurately for small particles which are not in rapid motion.

B. Calculation of Reaction Rate Controlled by Solid-state Processes

The isothermal oxidation of Zircaloy was shown to be approximately parabolic in 2 previous studies.<sup>(4,14)</sup> The parabolic rate law is usually considered to apply when the reaction rate is controlled by solid-state diffusion. The diffusion of either metal ions or oxide ions through the crystal lattice of the oxide film is usually the slow step. If there are no ageing effects in the oxide film, the rate of increase of oxide film thickness  $(x_0 - x)$  will be inversely proportional to the film thickness:<sup>(28)</sup>

$$\frac{d(x_0 - x)}{dt} \propto \frac{1}{(x_0 - x)} \quad (8)^*$$

It is also well established that the Arrhenius equation adequately describes the effect of temperature on the reaction rate for many metals.<sup>(28)</sup> The rate equation can then be expressed in terms of the surface temperature  $T_s$  as follows:

$$-\frac{dx}{dt} \propto \frac{1}{(x_0 - x)} \exp\left(-\frac{\Delta E}{RT_s}\right) \quad (9)$$

---

\*The usual form of the parabolic rate law is obtained by integrating at constant temperature to yield  $(x_0 - x)^2 \propto t$ .

If the pre-exponential factor of the rate equation,  $A$ , is expressed in units of milligrams of metal/sq cm, quantity squared per second, the parabolic rate law becomes:

$$-\left(\frac{dx}{dt}\right)_{\text{parabolic}} = \frac{10^{-6} A}{2\rho_m^2 (x_0 - x)} \exp\left(-\frac{\Delta E}{RT_s}\right) \quad (10)$$

The simple parabolic rate law as expressed in Equations 8, 9, and 10 does not apply precisely for spheres. The simple law ignores the fact that solid-state diffusion rates are altered by the changing area normal to diffusion as the thickness of the oxide layer becomes an appreciable fraction of the sphere radius. The difference in rates is less than 10% until 25% of the sphere has been reacted. The effect was, therefore, ignored in the present derivation. The equations describing this effect are derived in Appendix B.

### C. Calculation of Heat Transfer Rates of Reacting Metal Spheres in Water

The temperature-time history of reacting metal spheres in a water environment is influenced by the heat generated by chemical reaction and by heat losses by convection and radiation from the sphere to the water.

Convection heat loss rates can be formulated in terms of Newton's Law of cooling as follows:

$$H_{\text{CONV}} = h(4\pi x_0^2)(T_s - T_w) \quad (11)$$

The heat transfer coefficient  $h$  can be expressed in terms of a Nusselt number as follows:

$$\text{Nu} = h(2x_0)/k_f \quad (12)$$

The thermal conductivity  $k_f$  refers to a steam-hydrogen mixture at the mean film temperature. There are no experimental data over the temperature range of interest. Only approximate methods of direct calculation are available in the literature. A very useful procedure exists, however, to relate heat transfer rates and diffusion rates when they occur simultaneously. The relation is called the Lewis equation<sup>(26)</sup> and has the following form:

$$h_d = h/\rho_f C_{pf} \quad (13)$$

This applies if the diffusion coefficient of the gas mixture is numerically equal to the thermal diffusivity  $k_f/\rho_f C_{pf}$ . An estimate of the thermal diffusivity for an equimolar hydrogen-steam mixture at 1600 K was made by

a method given by Hirschfelder et al.<sup>(29)</sup> The calculated value is compared with the diffusion coefficient obtained from Equation 4 as follows:

$$\text{Thermal diffusivity at 1600 K} = \frac{12.1}{P} \text{ sq cm/sec} ;$$

$$\text{Diffusion coefficient at 1600 K} = \frac{15.8}{P} \text{ sq cm/sec} .$$

The agreement was considered sufficiently close to justify use of the Lewis relation to calculate rates of convective heat loss. The Lewis relation has the advantage that it applies for turbulent exchange whether numerical equality obtains or not. It can also be shown that the Nusselt numbers for gaseous diffusion and heat transfer are identical under these conditions.

The density of vapor to be used in Equation 13 was obtained from the gas laws as follows:

$$\rho_f = \frac{P}{\frac{1}{2} R(T_s + T_w)} , \quad (14)$$

and the specific heat of hydrogen-steam mixtures was approximated as follows:

$$C_{pf} = C_{pfo} \left( \frac{T_s + T_w}{2} \right)^{0.20} , \quad (15)*$$

where

$$C_{pfo} = 2.22 \text{ (cal)/(mole)(K}^{1.20}) .$$

Substituting Equations 13, 14, and 15 into Equation 11 yields

$$H_{\text{CONV}} = h_d \frac{P C_{pfo}}{R} \left( \frac{T_s + T_w}{2} \right)^{-0.80} (4\pi x_0^2)(T_s - T_w) , \quad (16)$$

and  $h_d$  can be eliminated in terms of Equations 2 and 4 to yield

$$H_{\text{CONV}} = \text{Nu} \frac{4\pi D_0 C_{pfo}}{R 2^{1.88}} x_0 (T_s + T_w)^{0.88} (T_s - T_w) . \quad (17)$$

The radiation heat loss is given by the Stefan-Boltzmann equation as follows:

$$H_{\text{RAD}} = \epsilon \sigma (4\pi x_0^2)(T_s^4 - T_w^4) , \quad (18)$$

where  $4\pi x_0^2$  is the spherical area.

---

\* Data were computed from Ref. 30, assuming an equimolar mixture.



Heat generated by reaction is proportional to the reaction rate, which is equal to the product of the surface area of unreacted metal,  $4\pi x^2$ , at any time and the rate at which the oxidation front moves into the metal:

$$H_{\text{REAC}} = Q \rho_m 4\pi x^2 \left( -\frac{dx}{dt} \right) \quad (19)$$

The foregoing heat generation and loss terms can be combined into an overall heat balance as follows: the rate of change of the metal temperature is proportional to the rate of heat generation less the rate of heat loss, or

$$C_{\text{pm}} \rho_m \left( \frac{4}{3}\pi x_0^3 \right) \frac{dT_m}{dt} = H_{\text{REAC}} - H_{\text{CONV}} - H_{\text{RAD}} \quad (20)$$

where  $\frac{4}{3}\pi x_0^3$  is the volume of the sphere.

Equation 20 does not describe the heat balance when the metal temperature reaches the melting point. At that point, heat is absorbed or evolved without a change in metal temperature. Allowance for this was made by using the following expression at the melting point:

$$L \rho_m \left( \frac{4}{3}\pi x_0^3 \right) \frac{dF}{dt} = H_{\text{REAC}} - H_{\text{CONV}} - H_{\text{RAD}} \quad (21)$$

where  $F$  is the fraction of original metal melted. For a computation in which the metal temperature is decreasing toward the melting point, Equation 21 would be used when the metal temperature reached 1852 C. The variable  $F$  would have an initial value equal to the fraction of original metal that had not yet reacted,  $(x/x_0)^3$ . Equation 21 would then be used until  $F$  reached zero, corresponding to a fully solidified particle. Further computation would be made on the basis of Equation 20 as the temperature continued to decrease.

It was assumed, for simplicity, that the radius of the sphere,  $x_0$ , was constant throughout the reaction and equal to the initial radius of unreacted metal. This ignores the fact that the sphere gains weight during the reaction and that the density of oxide is less than that of the metal. The volume increase of a completely reacted particle is the Pilling-Bedworth ratio,\* which is 1.56 for zirconium. The radius of the sphere would therefore increase by a factor equal to the cube root of 1.56 or only 16%. The specific heat and density of the spherical particles were

---

\*Ratio of the molar volume of  $\text{ZrO}_2$  to that of  $\text{Zr}$ .

also considered to be constant throughout the reaction. Actually, the specific heat would increase while the density would decrease. The error in one assumption is partially cancelled by the other.

#### D. Calculation of Temperature Drop Across the Oxide Film

Some authors have emphasized the importance of the heat-insulating effect of the oxide film on metal-gas reactions.<sup>(12)</sup> This is a very complicated factor to formulate precisely. A first approximation to describe this effect is to equate the heat flux from the surface by convection and radiation to the equation for steady-state heat conduction through a spherical shell of inner radius  $x$  and outer radius  $x_0$  (see Eckert,<sup>(26)</sup> page 25).

$$H_{\text{CONV}} + H_{\text{RAD}} = 4\pi k_{\text{ox}} \frac{x_0 x}{x_0 - x} (T_m - T_s) \quad (22)$$

#### E. Summary of Equations

The final equations used in the computer studies are summarized as follows (groups of constants are represented by symbols which are defined in Table 2):

Diffusion Rate:

$$-\left(\frac{dx}{dt}\right)_{\text{diffusion}} = \frac{Kx_0}{x^2} (T_s + T_w)^{0.68} \frac{\Delta P_w}{P} \quad (23)$$

Parabolic Rate Law:

$$-\left(\frac{dx}{dt}\right)_{\text{parabolic}} = \frac{B}{x_0 - x} \exp\left(-\frac{G}{T_s}\right) \quad (24)$$

Rates are computed from Equation 23 and Equation 24. The reaction is assumed to follow whichever rate is slower at any time.

Heat Balance:

$$Wx_0^3 \frac{dT_m}{dt} = Nx^2 \left(-\frac{dx}{dt}\right) - Yx_0^2(T_s^4 - T_w^4) - Ux_0(T_s + T_w)^{0.88}(T_s - T_w) \quad (25)$$

At the melting point,

$$L^1 x_0^3 \frac{dF}{dt} = Nx^2 \left(-\frac{dx}{dt}\right) - Yx_0^2(T_s^4 - T_w^4) - Ux_0(T_s + T_w)^{0.88}(T_s - T_w) \quad (26)$$

Temperature Drop through Oxide Film:

$$Z \frac{x_0 x}{x_0 - x} (T_m - T_s) = Y x_0^2 (T_s^4 - T_w^4) + U x_0 (T_s + T_w)^{0.88} (T_s - T_w) \quad (27)$$

Table 2

DEFINITION OF CONSTANTS USED IN  
COMPUTER STUDIES

$$K = \left( \frac{D_0 M_m}{2^{1.68} R n \rho_m} \right) Nu$$

$$Y = 4\pi Q \rho_m$$

$$B = \frac{10^{-6} A}{2 \rho_m^2}$$

$$U = \left( \frac{4\pi D_0 C_{pfo}}{2^{1.88} R} \right) Nu$$

$$G = \Delta E / R$$

$$L^1 = \frac{4}{3} \pi L \rho_m$$

$$W = \frac{4}{3} \pi C_{pm} \rho_m$$

$$Z = 4\pi k_{ox}$$

$$N = 4\pi Q \rho_m$$

## V. RESULTS OF ANALOG COMPUTER STUDY

The equations describing metal-water reactions, developed in the preceding chapter, were programmed on the PACE Analog Computer. The programming procedures are described in detail in Appendix C. Absolute temperatures, K, were used in the theoretical studies; however, the tabulated results are given in degrees, C.

### A. Metal Property Values

The values of the constants used in the computer study are given in Table 3. The specific heat and heat of reaction of zirconium were deduced from data compiled by Glassner.<sup>(31)</sup> Accordingly, a value of 8.0 cal/(mole)(K) was taken as the specific heat of zirconium over the temperature range from 1750 to 3900 K. Heat of reaction varied irregularly with temperature because of phase transitions. An average value of -140.5 kcal/mole\* was taken as the heat of reaction of molten zirconium with steam.

Table 3

#### VALUES OF CONSTANTS USED IN COMPUTER STUDIES

$C_{pm}$	specific heat of metal, 8.0 cal/(mole)(K)
$k_{ox}$	thermal conductivity of oxide, 0.006 cal/(sec)(cm)(K)
$L$	heat of fusion of metal, 4900 cal/mole
$M_m$	atomic weight of metal, 91.22 g/atom
$n$	moles of hydrogen generated per atom of metal reacted, 2
$Q$	heat of reaction, 140.5 kcal/mole
$R$	gas constant, 1.987 cal/(mole)(K); 82.06 (cc)(atm)/(mole)(K)
$\rho_m$	metal density, 6.5 g/cc
$\sigma$	Stefan Boltzmann constant, $1.37 \times 10^{-12}$ cal/(sec)(sq cm)(K <sup>4</sup> )

Studies of the emissivity of oxidized zirconium were reported by Lemmon.<sup>(14)</sup> Most of these studies were made with the oxygen uniformly distributed within the metal. Measurements made immediately after oxidation, before the oxide film could dissolve in the metal, gave a maximum value of 0.67 at the test temperature of 800 C. It appeared likely that this was a minimum value because of the transient character of oxide films on zirconium in a vacuum environment at high temperature. It was therefore decided to use the maximum emissivity of 1.0 for the computations. It was expected that this would lead to some cancellation of errors in the heat-loss calculations because the Nusselt number ( $Nu = 2$ ) chosen to represent convection cooling rates was the theoretical minimum value.

\*Value of heat of reaction at room temperature is -145.9 kcal/mole.

## B. Trial-and-error Computation of the Rate Constant at 1852 C

The only unknown factors remaining in the equations are the 2 constants of the parabolic rate law,  $A$  and  $\Delta E$ , and the ratio  $\Delta P_w/P$ . This latter ratio should be unity for runs in heated water when no significant quantity of inert gas is present. Under these conditions, the vapor pressure of water at the water-gas interface (see Figure 12) is equal to the total pressure.

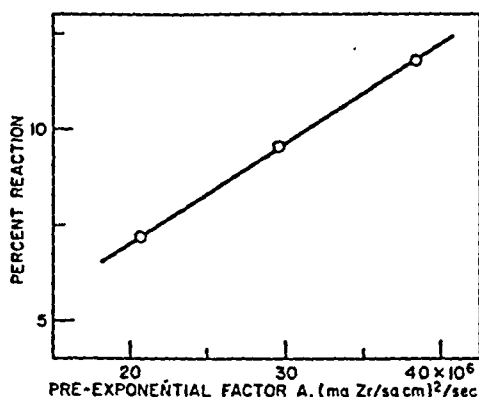
Calculations were made with assumed values of  $A$  and  $\Delta E$  for the case of solid metal spheres at the melting temperature [ $T_s(i) = 1852$  C,  $F(i) = 0.0$ ]. A sphere of diameter 0.21 cm ( $x_0 = 0.105$  cm) was used for the calculations because spheres of this diameter have the same surface-to-volume ratio as the 60-mil wires used in the experimental studies. The experimental value for the extent of metal-water reaction under these conditions was about 8 percent reaction.

Trial runs with the computer were made with assumed values of  $\Delta E$  of 35, 45, and 55 kcal/mole. The value of  $A$  was varied at constant  $\Delta E$  until the computed extent of reaction was within the range of experimental values.\* The effect of  $A$  on the computed extent of reaction is indicated in Figure 13 for an assumed energy of activation of 45 kcal/mole. The results in the figure indicate that the total extent of reaction is very sensitive to the value of  $A$  used in the calculation. The computed temperature-time and extent of reaction-time curves are given in Figure 14 for 35 and 55 kcal/mole. The numerical results are given in Table 4. The temperature-time curves in Figure 14 indicate that the course of the reaction is nearly independent of the value assumed for the activation energy  $\Delta E$  for these initial conditions.

Figure 13

### VARIATION OF THE COMPUTED EXTENT OF REACTION WITH PRE-EXPONENTIAL FACTOR

Assumed Activation Energy, 45 kcal/mole



#### Initial Conditions

Sphere Diameter:	0.21 cm
Metal Temperature:	1852 C
Physical State:	Solid
Heated Water:	$\Delta P_w/P = 1$

\* Preliminary experimental data indicated values of 9 to 9.5% reaction rather than the 8% quoted above.

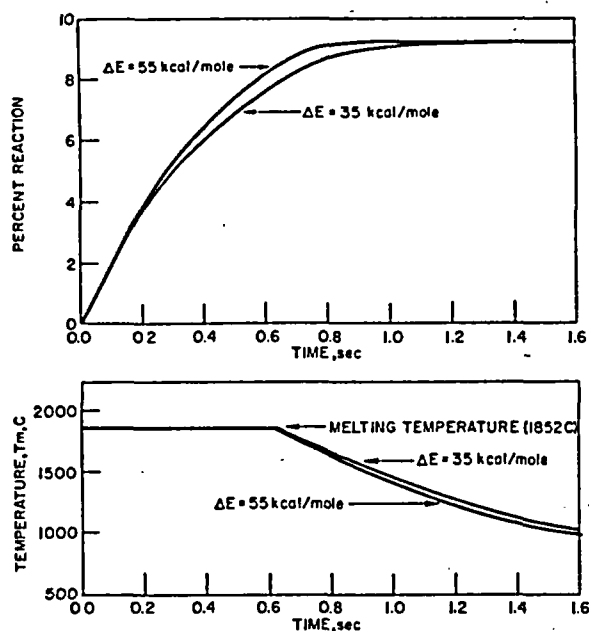


Figure 14  
COMPUTED REACTION AND TEMPERATURE FOR TWO VALUES OF ACTIVATION ENERGY

Table 4

COMPUTED RESULTS FOR ASSUMED VALUES OF  
ACTIVATION ENERGY

Initial Conditions

Sphere Diameter: 0.21 cm  
Metal Temperature: 1852 C  
Physical State: solid  
Heated Water:  $\Delta P_w/P = 1$

Activation Energy $\Delta E$ , kcal/mole	Value of A Required to Produce 9% Reaction (mg Zr/sq cm) <sup>2</sup> /sec	Rate Constant <sup>a</sup> at 1852 C, (mg Zr/sq cm) <sup>2</sup> /sec
35	$2.52 \times 10^6$	633
45	$29.5 \times 10^6$	695
55	$316 \times 10^6$	695

$$^a \text{Rate Constant} = A \exp \left( \frac{-\Delta E}{RT} \right)$$

A more detailed study of the computer solution for one particular case is given in Figure 15. The diffusion-limited and the parabolic law-limited reaction rates are included in the figure. The computer responds to whichever rate is lowest at any given time. The initial reaction is controlled by diffusion; heat is produced at a greater rate than it is lost.

The heat is absorbed in the melting process. Before melting is complete, however, the reaction becomes controlled by the parabolic rate law, and the reaction slows down. The specimen begins to lose heat at a greater rate than it is being generated, and freezing occurs. Finally, rapid cooling occurs after the sample has fully solidified. The greater part of the reaction occurs isothermally at 1852 C under these conditions. The reaction rate constant,  $A(\exp - \Delta E/RT)$ , at 1852 C required to produce 9% reaction is nearly independent of the value assumed for the activation energy  $\Delta E$ , as shown in the final column of Table 4.

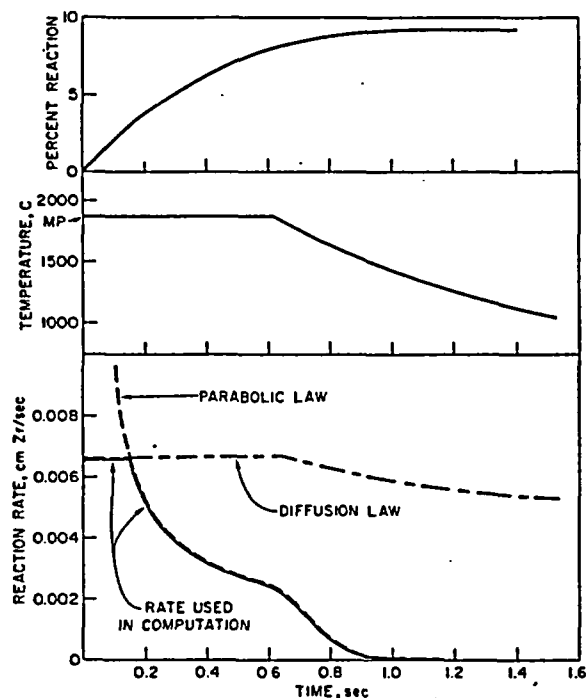


Figure 15

### COMPUTER SOLUTION FOR REACTIONS OF ZIRCONIUM SPHERE WITH WATER

Activation Energy: 45 kcal/mole

#### Initial Conditions

Sphere Diameter: 0.21 cm  
Metal Temperature: 1852 C  
Physical State: Solid  
Heated Water:  $\Delta P_w/P = 1$

#### C. Comparison of Rate Constants with Those of Previous Investigators

Values of 633 to 695 (mg Zr/sq cm)<sup>2</sup>/sec, depending on the value of the activation energy, were obtained for the constant of the parabolic rate law at 1852 C in the previous section. It was of interest to compare these values with those reported by previous investigators. Studies of the reaction of Zircaloy-2 with water, reported by Bostrom,<sup>(4)</sup> and studies of the reaction with steam, reported by Lemmon,<sup>(14)</sup> were examined in particular. Neither investigator considered the possibility that the reaction might have been limited by gaseous diffusion during the early part of a run. Results reported by Bostrom at 1750 C deviated seriously from the parabolic slope on a plot of the log of hydrogen gas evolved vs the log of time. The reaction appeared to be somewhere between parabolic and linear. A careful analysis of this and other runs indicated that the deviation from the parabolic slope might have been due to an initial rate which was lowered

because of a diffusion limitation or for other reasons.\* A method of obtaining the parabolic rate constant from such data is outlined in Appendix D.

The resulting rate constants are plotted as a function of reciprocal temperature in Figure 16. The reaction rate at the melting point obtained from the condenser-discharge studies is also included on the figure. The falling-off of the Battelle data above 1300 C is not understood. The value obtained from the condenser-discharge studies is more in line with Bostrom's data. The line drawn in Figure 16 corresponds to an activation energy of 45.5 kcal/mole and fits condenser-discharge data, Bostrom's data, and the low-temperature Battelle data. The activation energy obtained in this way was used for further computer studies. The integrated form of the rate law, determined in this way, is as follows:

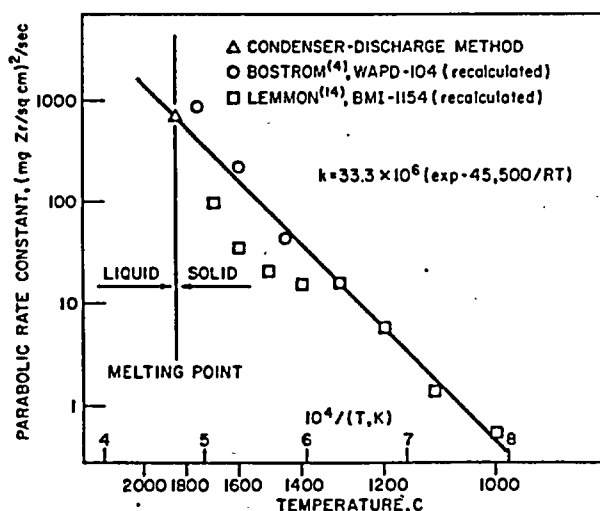
$$w^2 = 33.3 \times 10^6 t \exp \left( - \frac{45,500}{RT} \right) ,$$

where  $w$  is the weight of zirconium reacted per unit surface area in mg/sq cm and  $t$  is time in sec. The rate law expressed in the units employed in the Battelle studies becomes

$$V^2 = 4.82 \times 10^8 t \exp \left( - \frac{45,500}{RT} \right) ,$$

where  $V$  is the volume of hydrogen at standard conditions evolved per unit surface area in cc  $H_2$  (STP)/sq cm, and  $t$  is time in min.

Figure 16  
EFFECT OF TEMPERATURE ON THE  
ZIRCONIUM-WATER REACTION



\*A lag in bringing the specimen to temperature might produce a similar effect.



#### D. Calculation of Reaction in Heated Water

Tentative values of the constants of the parabolic rate law were determined in the previous section by reference to a single set of experimental results in heated water and by reference to isothermal studies of 2 previous investigators.

##### 1. Effect of Variations of the Emissivity and the Nusselt Number

Several additional calculations were made for solid spheres of 0.21-cm diameter at the melting temperature; the constants determined in the previous section were used. Increasing the Nusselt number to 3 decreased the extent of reaction from 9.55 to 8.65%. Decreasing the emissivity from 1 to 0.75 increased the reaction from 9.55% to 11.4%. The variations of emissivity and Nusselt number altered the results only slightly more than the uncertainty in the experimental results.

##### 2. Effect of Initial Temperature and Particle Size

It remains to compute results for a variety of initial metal temperatures and particle sizes and compare them with experimental results. Complete computed results for runs in heated water ( $\Delta P_{H_2O}/P = 1$ ) are summarized in Table 5. Computed temperature-time and percent reaction-time curves for spheres of diameter 0.21 cm are plotted in Figure 17 for a series of initial metal temperatures.

Table 5  
COMPUTED RESULTS FOR THE REACTION OF  
ZIRCONIUM SPHERES WITH HEATED WATER  
( $\Delta P_{H_2O}/P = 1.0$ )

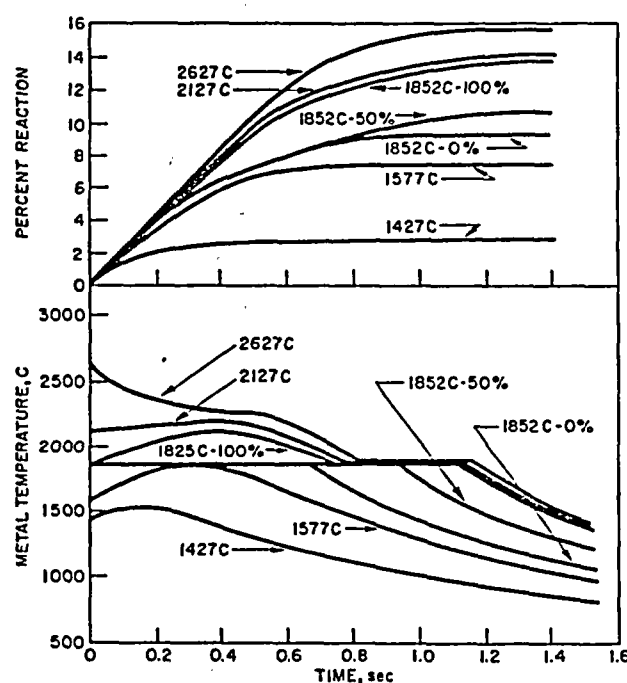
Sphere Diameter, cm	Initial Metal Temperature		Initial Physical State	Peak Metal Temperature, C	Time for Reaction to Reach One-half of Final Value, sec	Time to Cool to 1500 K (1227 C), sec	Final Extent of Reaction, %
	K	C					
0.21	1700	1427	Solid	1500	0.12	0.61	2.85
0.21	1850	1577	Solid	1852	0.20	1.04	7.55
0.21	2125	1852	Solid	1852	0.26	1.24	9.25
0.21	2125	1852	50% Liquid	1852	0.31	1.50	10.65
0.21	2125	1852	Liquid	2120	0.35	1.68	13.8
0.21	2400	2127	Liquid	2200	0.36	1.70	14.5
0.21	2900	2627	Liquid	2627	0.32	1.73	15.7
0.105	2125	1852	Solid	1852	0.12	0.56	13.4
0.105	2125	1852	Liquid	2800	0.23	0.81	39.3
0.105	2400	2127	Liquid	2800	0.22	0.81	39.5
0.105	2900	2627	Liquid	2800	0.22	0.81	39.6
0.052	2125	1852	Solid	3550	0.100	0.33	69.2
0.052	2125	1852	Liquid	3550	0.095	0.32	69.2
0.052	2400	2127	Liquid	3550	0.094	0.32	69.2
0.052	2900	2627	Liquid	3550	0.090	0.31	69.3
0.026	2125	1852	Liquid	4300	0.042	0.095	84.2
0.026	2400	2127	Liquid	4300	0.042	0.095	84.2
0.026	2900	2627	Liquid	4300	0.042	0.095	84.2

The results show that the metal temperature is able to rise considerably above the melting temperature when the metal is fully melted initially. A run with an initial temperature of 2127 C showed only a slight temperature rise. A run with an initial temperature of 2627 C showed an immediate temperature decrease, reaching a level of about 2200 C. An examination of the equations showed that, so long as the reaction is diffusion controlled, there is an equilibrium temperature at which the rates of heat generation balance the rate of heat loss. The temperature would remain nearly constant until 100 percent of the metal reacted if it were not for the rate decrease caused by parabolic rate law.

Figure 17

COMPUTED REACTION AND TEMPERATURE  
FOR 0.21-cm-DIAMETER ZIRCONIUM SPHERES  
IN HEATED WATER

(Curve Labels are Initial Metal Temperatures  
and Percentages of Metal Melted)

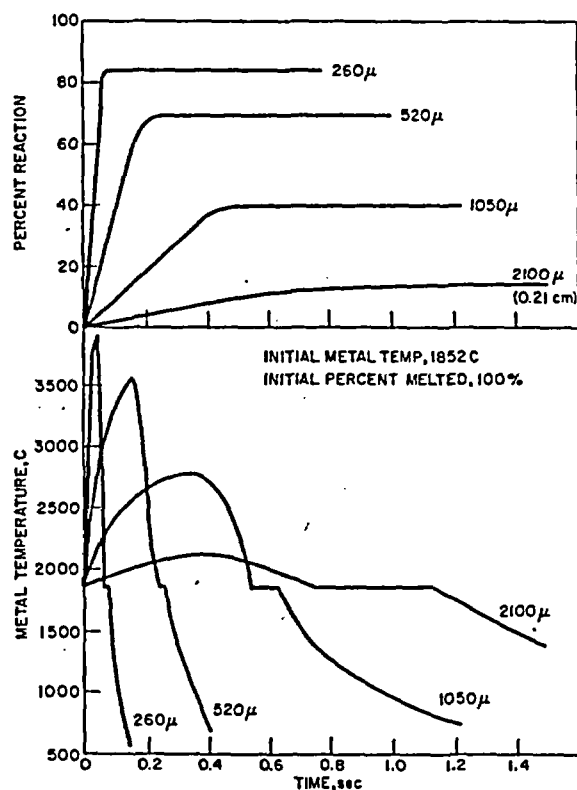


Computations were also made for sphere diameters of 0.105, 0.052, and 0.026 cm. The temperature-time and the extent of reaction-time curves are plotted in Figure 18 for the case of fully melted spheres initially at the melting point. The results predict that reaction rates increase greatly with decreasing particle size. The time required to complete one-half of the final extent of reaction is listed for all of the computed runs in Table 5. The times required for the particles to cool to 1227 C (1500 K) are also listed in the table. The 1500 K temperature

was chosen arbitrarily as a temperature below which little if any reaction occurs. It also approximates the temperature at which particles no longer appear luminous on the high-speed motion picture film used in experimental studies.\*

Figure 18  
COMPUTED EXTENTS OF REACTION AND  
TEMPERATURES FOR MOLTEN  
ZIRCONIUM SPHERES IN  
HEATED WATER

(Numbers Indicate Sphere Diameters)



The computed curve for a particle diameter of 0.052 cm is one of those given in Figure 18. Computed results for a series of initial metal temperatures are given in Table 5 and indicate that the temperatures rapidly approached the equilibrium value of 3550 C regardless of the initial metal temperature, even for initially solid metal at the melting point. Rapid cooling occurred as soon as the rate determined by the parabolic law assumed control of the reaction. The result is that the final extent of reaction (69.2%) is independent of the initial metal temperature.\*\*

\*Typical film sequences are shown in Ref. 1.

\*\*The lowest temperature investigated for this case was 1852 C with the metal initially solid. The extent of reaction would decrease sharply at some lower initial temperature.

### 3. Temperature Drop Across the Oxide Film

The temperature drop across the oxide film was described, approximately, by Equation 27, Chapter IV. The metal temperature  $T_m$  was recorded on the computer curves, and the surface temperature  $T_s$  determined the reaction rate and the heat loss rate. Computations indicated that the temperature drop,  $T_m - T_s$ , was significant only after considerable reaction had occurred, i.e., when a thick oxide film was present. Particles having a diameter of 0.21 cm reacted only to the extent of about 15% (see Figure 18). The maximum temperature drop during these runs was about 35 C and occurred while the metal was cooling through the melting point. Particles having a diameter of 0.105 cm reacted to the extent of 40% and had a maximum temperature drop of the order of 100 C. Finer particles reacted to a still greater extent and had correspondingly greater differences between the metal temperature and the surface temperature.

An assumption that the metal was always at the same temperature as the oxide surface would have changed the computed results slightly. No important changes in the character of the results, however, would have occurred.

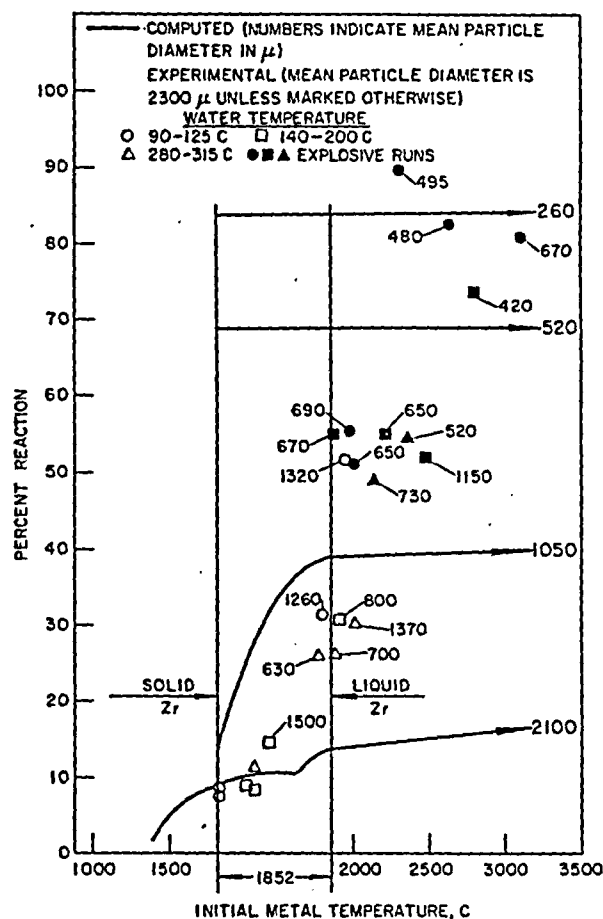
### 4. Comparison of Computed Extent of Reaction with Experimental Values

Computed results for final extent of reaction are plotted as a function of initial metal temperature for the particle sizes studied in Figure 19. Experimental points for runs in heated water are included on the figure. Numbers adjacent to the points are the measured mean particle diameters. The results show that the experimental points fall generally within the ranges defined by the computations. The computed results in Figure 19 indicate that only slightly more reaction occurs with metal heated to very high temperatures than that occurring with metal at the melting point so long as the metal is fully melted initially.

Experimental data for runs in heated water were plotted as a function of the particle diameter in Figure 9. The theoretical curve on the figure is the computed extent of reaction for fully melted metal at the melting point. This curve would differ very little from one based on higher initial metal temperatures. The comparison between the experimental points and the theoretical curve seems satisfactory. Experimental runs in which the metal was not fully melted (particle diameter of 2300  $\mu$ ) understandably had less total reaction than values indicated by the theoretical curve.

Figure 19

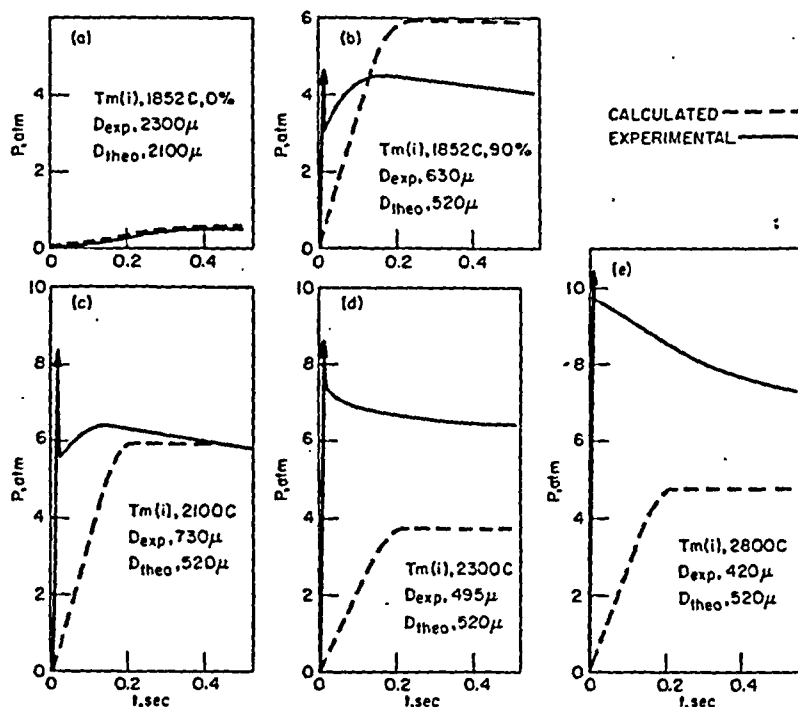
COMPARISON OF COMPUTED AND  
EXPERIMENTAL RESULTS OF  
ZIRCONIUM RUNS IN  
HEATED WATER



5. Comparison of Computed Reaction Rates with Experimental Pressure Traces

Experimental pressure traces were plotted in Figure 7 for runs in heated water. These are replotted in Figure 20 along with the computed extent of reaction vs time curves obtained with values of initial metal temperature and particle diameter similar to those of the experiment. The rate curves were almost identical when the metal was not melted (see Figure 20a). It was pointed out previously that experimental pressure traces appeared to be composites of a slow reaction and a very rapid reaction for runs in the molten metal range. It is evident from the figure that the computations do not predict the rapid reactions which are observed in the more energetic runs.

Figure 20

COMPARISON OF EXPERIMENTAL AND THEORETICAL  
PRESSURE-TIME CURVES FOR RUNS IN HEATED WATER

An examination of the equations showed that the Nusselt number is the principal factor controlling the reaction rate in the early stages of reaction. It was also evident that a considerable increase over the minimum value of 2 would be required to account for high observed rates. The effect of a large increase in Nusselt number was investigated on the computer for a large particle (diameter of 0.508 cm) with the use of 55 kcal/mole for the activation energy. The results, shown in Table 6, indicate the time to complete one-half of the reaction is decreased by a factor of 5 when the Nusselt number is increased from a value of 2 to a value of 16. The total extent of reaction is relatively unaffected by changes up to  $Nu = 8$ , but decreases somewhat at still higher values.

It is important at this point to consider the causes of an increased Nusselt number (increased diffusion rate). Nusselt numbers increase when there is rapid motion or increased turbulence.\* It, therefore, seemed likely that the reacting particles were in rapid motion in runs that showed the rapid pressure rise. This was confirmed when high-speed "streaks" indicative of rapid particle motion were noted on the Fastax motion pictures of runs in room-temperature water. The streaks were

\*Rapid motion or turbulence physically removes the hydrogen blanket surrounding particles and would thereby increase the rate of both the diffusion and cooling processes.

not present on films taken of identical discharge runs made in an argon gas environment or in less energetic runs in water that had slow pressure rises. The lengths of streaks indicated particle velocities of the order of 20 to 50 ft/sec.

Table 6

EFFECT OF NUSSELT NUMBER ON THE REACTION  
RATE FOR A LARGE PARTICLE

Initial Conditions

Sphere Diameter: 0.508 cm (0.2 in.)  
Metal Temperature: 1852 C  
Physical State: solid  
Heated Water:  $\Delta P_w/P = 1$   
Activation Energy: 55 kcal/mole

Nusselt Number	Time for Reaction to Reach One-half of Final Value, sec	Time to Cool to 1500 K (1227 C), sec	Final Extent of Reaction, %
2	1.10	4.10	6.85
4	0.60	3.40	7.00
8	0.39	2.45	7.40
12	0.28	1.82	5.70
16	0.24	1.41	4.63

Rapid particle motion could have been caused initially in energetic runs by momentum imparted to particles by the electrically exploded wire. The streaks, however, persisted for several milliseconds even though the discharge required only 0.3 msec. It was most likely that the reaction process itself was responsible for sustaining particle motion. Apparently, the rapid evolution of hydrogen was able to provide a thrust which propelled particles rapidly and irregularly through the water. Particle motion would, therefore, slow markedly when the reaction passed from the diffusion-controlled regime to the slower kinetically controlled regime. It would not be correct, then, to compute the reaction on the basis of an increased Nusselt number for an entire run. It would be more nearly correct to relate the Nusselt number to the reaction rate in some way. It was believed, however, that such an additional complication would tend to obscure the interpretation of computed results.

The equations were examined to determine the effect of an increased Nusselt number only during the period of diffusion control. The time spent by the reaction in the diffusion regime would be decreased. The total extent of reaction, however, would be relatively unchanged. This

resulted from the fact that both the heat generation rate (diffusion rate) and the principal heat loss mechanism (for small particles), convection, were both increased equally by an increased Nusselt number.

It was assumed, therefore, that rapid reactions would reach the same final extent of reaction as they would if rapid particle motion had not occurred. The only effect of particle motion was to speed the reaction through the diffusion regime.

The appearance of a composite reaction in experimental runs suggested that only certain of the particles produced in runs are able to undergo the rapid reaction. This further suggested that there was a critical particle size. Particles smaller than the critical size are able to undergo rapid motion and therefore react rapidly. Larger particles undergo the slower reaction.

Experimental results shown in Figure 3 indicate that the critical particle diameter separating explosive and nonexplosive runs is ca  $500\ \mu$  in room-temperature water. Experimental results shown in Figure 9 indicate that the critical particle diameter is ca  $1000\ \mu$  (1 mm) in heated water. The lack of a sharp break in the extent of reaction corresponding to the critical diameters in Figures 3 and 9 tends to verify the assumption that the only effect of an increased Nusselt number is to speed the reaction through the diffusion regime.

#### E. Calculation of Reaction in Room-temperature Water

##### 1. Effect of Water Vapor Pressure

Experimental results showed that the extent of reaction of runs in room-temperature water was much less than in similar runs in heated water. The most likely cause of this was thought to be a decreased rate of gaseous diffusion resulting from the low vapor pressure of room-temperature water. It was shown in the calculation of the diffusion rate (see Equation 7, Chapter IV) that the diffusion rate is proportional to  $\Delta P_w/P$ , where  $\Delta P_w$  is the difference in water vapor pressure at the liquid water surface and the hot metal surface, and  $P$  is the total pressure. It was assumed that the metal reacts with all the water vapor reaching the metal surface so that the partial pressure of water vapor at the metal surface is zero. The quantity  $\Delta P_w$  is then equal to the vapor pressure of water at the water-water vapor interface. In most of the runs, there was no air or added inert gas, so that the vapor pressure of the water was also the total pressure. The term  $\Delta P_w/P$  would be unity. Consider the value of  $\Delta P_w/P$  after some metal-water reaction had occurred. A 10 percent reaction of the 60-mil specimen in either reaction cell would yield a hydrogen pressure of about 0.5 atm. If the water surface is assumed to remain at its original temperature, the following values of  $\Delta P_w/P$  would obtain at various water temperatures after 10% reaction:



Water Temp, C	Water Vapor Pressure, atm	$\Delta P_w/P$ after 10% Metal-Water Reaction <sup>a</sup>
25	0.03	0.057
100	1	0.67
200	15	0.97
300	85	0.99

<sup>a</sup> $\Delta P_w/P$  is equal to (vapor pressure)/  
(0.5 atm + vapor pressure) for these  
conditions.

The above table shows how the diffusion-limited reaction rate might be tremendously reduced in 25 C water, but not be seriously affected in heated water.

Computer calculations were then made as based on the assumption that the water surface temperature ( $T_{ws}$  in Figure 12) did not change during reaction. Results indicated that there should be virtually no reaction in room-temperature water. It was clear, then, that the water surface facing reacting particles does not remain at the bulk water temperature. The experimental fact of a decreased reaction in room-temperature water, however, indicated that the water does not reach the boiling point. Rather, the water surface temperature and the corresponding vapor pressure are intermediate between these 2 limits.

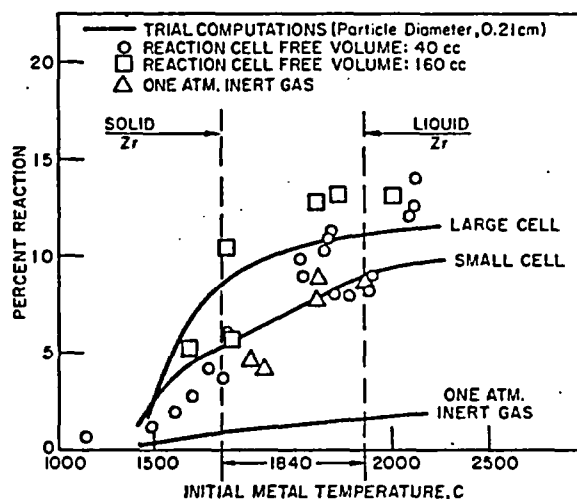
Two assumptions were tested on the computer. The first method assumed that the water surface temperature was an average of the bulk water temperature and the boiling point determined by the changing total pressure. This assumption required the insertion of vapor pressure data into the computation by means of a function generator. Computations were made for 3 cases with 60-mil specimens (particle diameter of 0.21 cm) in room-temperature water:

- 1) runs having a cell free volume of 40 cc and no added inert gas (normal runs);
- 2) runs with a free volume of 160 cc and no added inert gas; and
- 3) runs having 1 atm of added inert gas with 40-cc free volume.

The computed results are compared with experimental results in Figure 21. Increased cell volume increased the computed reaction because there was a lowered total pressure generated by the evolving hydrogen. Added inert gas decreased the computed reaction by raising the total pressure. The experimental results with added inert gas did not show the predicted decrease. The averaged-temperature method of computing the gaseous diffusion rate was therefore abandoned.

Figure 21

COMPARISON OF EXPERIMENTAL RESULTS  
WITH COMPUTED RESULTS BASED ON  
TEMPERATURE-AVERAGED DIFFUSION  
RATE FOR 60-mil WIRES IN ROOM-  
TEMPERATURE WATER



The second method of computing the term  $\Delta P_w/P$  was to assume that a constant fractional value applied throughout the reaction. Physically, this could be interpreted to mean that some of the water at the surface was heated to the boiling point by heat from the reacting particle and some of it was at the bulk water temperature. Surface turbulence might produce this kind of an alternation of boiling water and room-temperature water at any point on the surface. Table 7 shows the effect of assumed values of  $\Delta P_w/P$  on the computed extent of reaction. A value of unity for  $\Delta P_w/P$ , would correspond to runs in heated water. From this computation, it was determined that a value of  $\Delta P_w/P$  of 0.5 would reproduce experimental results of runs in room-temperature water.

Table 7

EFFECT OF VARIATIONS OF  $\Delta P_w/P$  ON THE EXTENT OF REACTION OF 0.21-cm ZIRCONIUM SPHERES  
(Activation Energy: 55 kcal/mole)

Initial Metal Temperature, C, and Physical State	Assumed Value of $\Delta P_w/P$	Final Extent of Reaction, %		Initial Metal Temperature, C, and Physical State	Assumed Value of $\Delta P_w/P$	Final Extent of Reaction, %	
		Computed	Exp			Computed	Exp
1852, solid	1.00	9.1	(5.0)	1852, liquid	1.00	18.6	(9.5)
1852, solid	0.72	7.7		1852, liquid	0.72	11.2	
1852, solid	0.52	4.5		1852, liquid	0.52	9.7	
1852, solid	0.37	3.3		1852, liquid	0.37	6.0	
1852, solid	0.26	2.3		1852, liquid	0.26	3.9	

## 2. Comparison of Computed Extent of Reaction with Experimental Values

Further computations were made with the value of 0.5 for  $\Delta P_w/P$ . All other parameters in the equations were identical with those used in the calculations of runs in heated water. It should be pointed out that the above pressure ratio affects only the diffusion-controlled reaction rate and not the heat loss rate or the parabolic-law-controlled reaction rate. Computed results for runs in room-temperature water (with  $\Delta P_w/P = 0.5$ ) are summarized in Table 8. Temperature-time and percent reaction-time curves for a particle of 0.21-cm diameter are plotted in Figure 22 for a series of initial metal temperatures. The results are similar in character to those obtained in heated water, although there is less total reaction under similar initial conditions. The effect of particle size is shown in Figure 23, in which computer curves are plotted for the case of fully melted metal at the melting point. The calculated reaction rates increase greatly with decreasing particle size in the same way as they did in heated water.

Table 8

COMPUTED RESULTS FOR THE REACTION OF ZIRCONIUM SPHERES WITH ROOM-TEMPERATURE WATER

( $\Delta P_w/P = 0.5$ )

Sphere Diameter, cm	Initial Metal Temperature		Initial Physical State	Peak Metal Temperature, C	Time for Reaction to Reach One-half of Final Value, sec	Time to Cool to 1500 K (1227 C), sec	Final Extent of Reaction, %
	K	C					
0.21	1700	1427	Solid	1470	0.15	0.55	2.25
0.21	1850	1577	Solid	1600	0.22	0.79	3.83
0.21	2125	1852	Solid	1852	0.24	1.01	5.45
0.21	2125	1852	50% Liquid	1852	0.39	1.24	7.4
0.21	2125	1852	Liquid	1852	0.48	1.49	9.2
0.21	2400	2127	Liquid	2127	0.52	1.68	10.3
0.21	2900	2627	Liquid	2627	0.53	1.74	10.8
0.105	2125	1852	Solid	1852	0.14	0.43	10.8
0.105	2125	1852	Liquid	1930	0.20	0.67	14.8
0.105	2400	2127	Liquid	2127	0.19	0.68	15.3
0.105	2900	2627	Liquid	2627	0.19	0.69	16.1
0.052	2125	1852	Solid	1852	0.057	0.21	16.6
0.052	2125	1852	Liquid	2280	0.086	0.28	27.8
0.052	2400	2127	Liquid	2300	0.086	0.28	28.5
0.052	2900	2627	Liquid	2627	0.085	0.28	29.6
0.026	2125	1852	Liquid	2730	0.070	0.11	54.5
0.026	2400	2127	Liquid	2730	0.070	0.11	54.7
0.026	2900	2627	Liquid	2730	0.070	0.11	54.8

Computed results for final extent of reaction are plotted as a function of initial metal temperature in Figure 24. Experimental points for runs in room-temperature water are included. Mean particle diameters corresponding to experimental points are also indicated. The comparison shows that the experimental points are reasonably consistent with the computed results.

Figure 22

COMPUTED REACTION AND TEMPERATURE FOR  
0.21-cm-DIAMETER ZIRCONIUM SPHERES  
IN ROOM-TEMPERATURE WATER

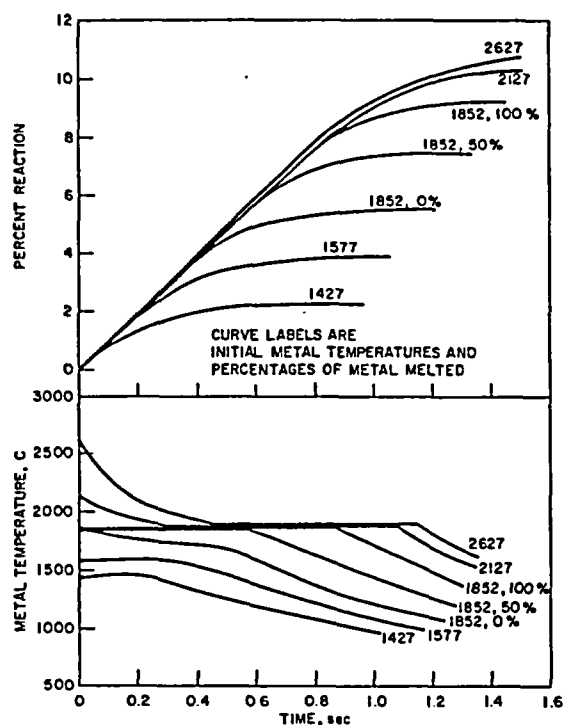


Figure 23

COMPUTED REACTION AND TEMPERATURE  
FOR MOLTEN ZIRCONIUM SPHERES IN  
ROOM-TEMPERATURE WATER

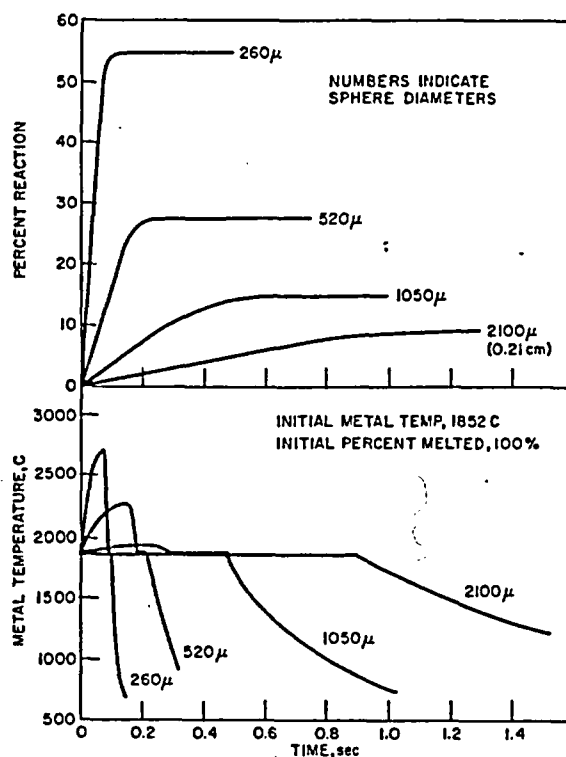
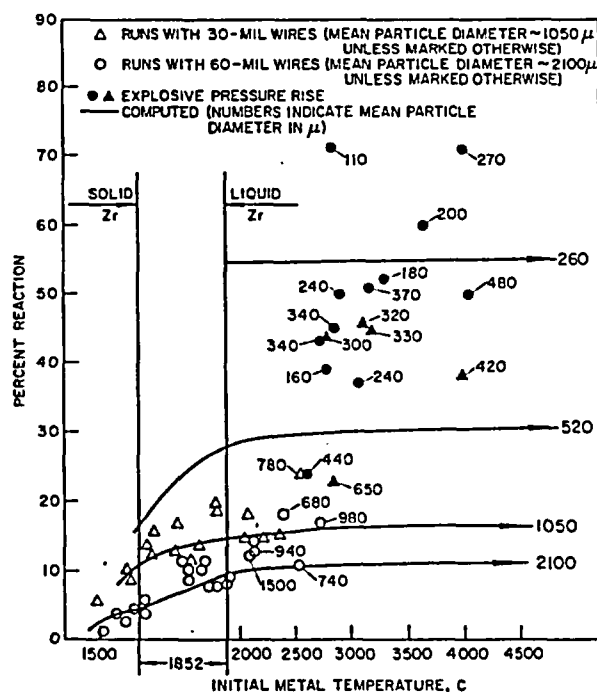


Figure 24

COMPARISON OF COMPUTED AND EXPERIMENTAL  
RESULTS OF ZIRCONIUM RUNS IN ROOM-  
TEMPERATURE WATER



Computed results in room-temperature water were relatively independent of initial metal temperature when the metal was fully melted initially, just as they were in the case of heated water. It was therefore advantageous to compare the experimental points with results computed for the case of fully melted metal initially at the melting point. The comparison, shown in Figure 3, shows excellent agreement. The experimental points corresponding to runs in which the specimen wires, either 30 or 60 mils in diameter (equivalent spherical diameters of 0.105 and 0.21 cm), were not fully melted would be expected to fall below the theoretical curve.

### 3. Comparison of Computed Reaction Rates with Experimental Pressure Traces

Experimental pressure traces (see Figure 2) are replotted in Figure 25 along with computed extent of reaction vs time curves. The computed curves were obtained with values of initial metal temperature and particle diameter similar to those of the experiment. The computed and experimental rate curves are similar in character when the reaction has the slow pressure rise. Reactions having explosive pressure rise rates were more rapid than computed rates. The reasons for this were discussed in detail in a previous section.

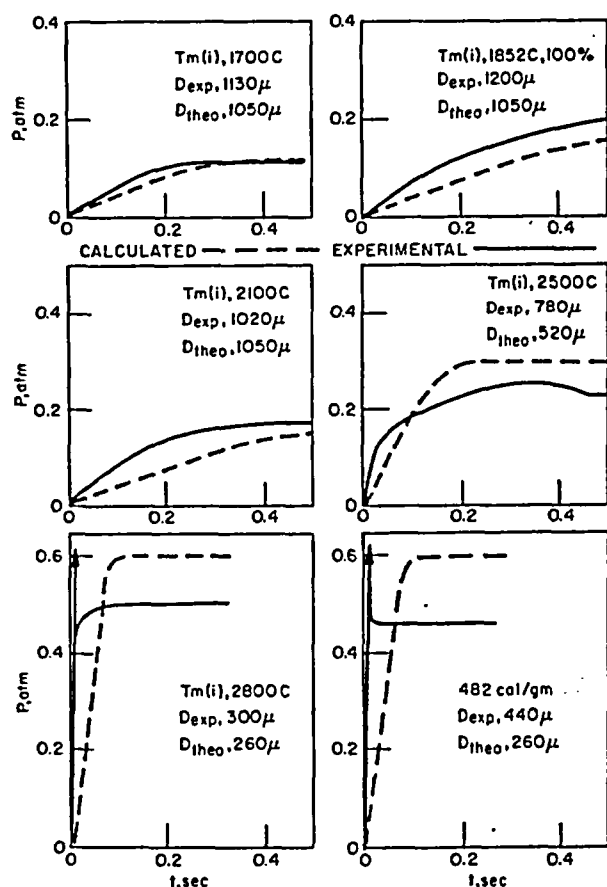


Figure 25  
COMPARISON OF EXPERIMENTAL  
AND THEORETICAL PRESSURE-  
TIME CURVES FOR RUNS IN  
ROOM-TEMPERATURE WATER

## VI. DISCUSSION OF RESULTS AND COMPARISON WITH PREVIOUS STUDIES

The combined experimental and theoretical study of the zirconium-water reaction has shown which chemical and physical processes are important to the course of the overall reaction and which are of secondary influence. The results will be shown to be fully consistent with those obtained by previous investigators.

### A. Reaction Scheme

Molten zirconium droplets coming into sudden contact with liquid water react very rapidly but to a negligible extent (less than 0.2 percent reaction) before the reaction rate becomes limited by a process of gaseous diffusion. This limitation arises from the formation of a gaseous bubble surrounding each particle. It is necessary for water vapor to diffuse through the steam-hydrogen bubble toward the metal droplet and for hydrogen to diffuse away from the metal. The diffusion process appears to be a quasi-steady-state process. An unreasonably large bubble would result from the continuous accumulation of hydrogen. Calculations of the minimum diffusion rates to a sphere gave initial reaction rates lower than those obtained from extrapolations of the parabolic rate law. As the oxide layer thickens, the reaction rate given by the parabolic law decreases until it becomes the slowest step in the reaction. This inevitably results in rapid cooling and quenching of the reaction.

A highly simplified mathematical model of the reaction was formulated and solutions were obtained on an analog computer. A number of simplifying assumptions were used in setting up the equation. It was anticipated that the computer solutions would represent the nominal behavior of hot zirconium spheres in water with a minimum of complication. Most of the simplifying assumptions would result in uncertainties only at high percentages of reaction. The principal assumptions were:

1. use of the simple parabolic rate law for spherical geometry;
2. assumption of constant particle radius throughout reaction;
3. assumption of constant specific heat and density of the particle;
4. approximate formulation of the temperature drop across the oxide film.

The wide range of agreement between calculated and experimental results (e.g., see Figure 3) indicated that the errors introduced by the simplifying assumptions were probably no greater than the experimental uncertainties.

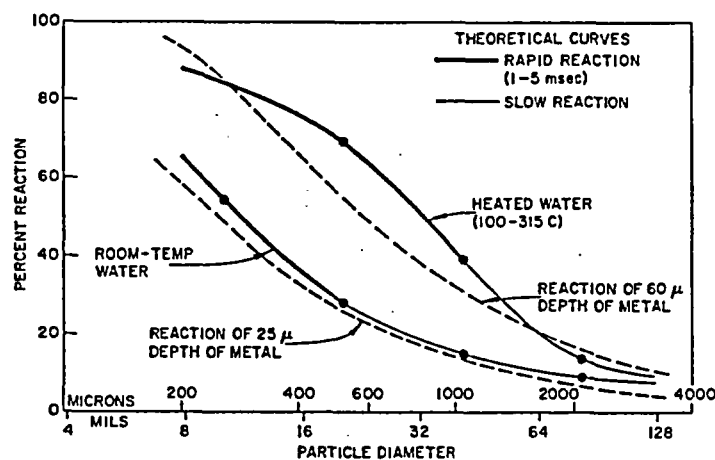
It was assumed implicitly that the oxide shell would not shatter and separate from unreacted metal as a result of the rapid temperature changes occurring during reaction. This assumption seems justified in view of the spherical character of particles and the uniformity of the oxide films.

### B. Total Extent of Reaction

The total extent of reaction of zirconium spheres suddenly brought into contact with water was found to depend primarily on the water temperature and the sphere diameter. The dependence was expressed in Figures 3 and 9. The theoretical curves are replotted in Figure 26. A similar curve was prepared in the Aerojet studies.<sup>(11)</sup> In that work, the particles produced by dumping a quantity of molten zirconium into water followed by dispersion with a blasting cap were sized and the extent of reaction of each particle determined. It was concluded that the results could be represented approximately by assuming that oxidation occurred to a depth of  $25\ \mu$  on each particle. The extent of reaction corresponding to  $25\text{-}\mu$  reaction is compared with the theoretical curves in Figure 26. The  $25\text{-}\mu$  curve is in good agreement with the theoretical curve for room-temperature water. This is to be expected, since the Aerojet work was carried out in room-temperature water. A curve based on  $60\text{-}\mu$  reaction is also plotted in Figure 26 and shows limited agreement with the theoretical curve for heated water.

Figure 26

#### EXTENT OF REACTION AS A FUNCTION OF PARTICLE DIAMETER FOR MOL- TEN ZIRCONIUM SPHERES FORMED IN WATER



The falling drop experiments reported by Battelle<sup>(14)</sup> used 0.2-in. (5000- $\mu$ ) Zircaloy-2 droplets. The thicknesses of oxide layer varied between 24 and 68  $\mu$  (corresponding to 2.7 and 5.8 percent reaction) irregularly as the water temperature was varied between 92 and 200 F. These values are also in agreement with Aerojet data and with the results of the present study.

The results of Milich and King<sup>(6)</sup> are also consistent with those of the present study. They dropped batches of molten metal into water under various conditions of temperature and pressure. Their results are more difficult to compare quantitatively because the effective particle sizes were uncertain and because the specimens were heated for a period of 6 to 8 sec in contact with water vapor. Their results are summarized briefly in Table 9. The large differences between reaction in room-temperature water and heated water were probably due to the reaction of steam with the samples while they were being heated. The reaction of zirconium with water vapor in a gaseous environment would also be controlled in large measure by gaseous diffusion. The reaction rate would depend on the partial pressure of water vapor and would increase as indicated in Table 9. It might be assumed that when inert gas was present very little reaction occurred before the sample was dropped into the water. The 1.3 to 2.6 percent reaction in room temperature water would then be reasonable for rather large particles.

Table 9

ZIRCONIUM-WATER REACTION STUDIES<sup>a</sup>  
by Milich and King<sup>(6)</sup>

Water Vapor Pressure, psia	Argon Pressure, psia	ml H <sub>2</sub> /g Zr	% Reaction <sup>b</sup>
0.5 <sup>c</sup>	200-1000	6.7-7.8	1.3-1.6
0.5 <sup>c</sup>	15	8.2-12.6	1.7-2.6
0.5 <sup>c</sup>	0	28-29	5.7-5.9
40-280	0	110-130	22-26
750	0	280	57

<sup>a</sup>From 2 to 10 g of molten zirconium at ~1852 C were dropped into 130 ml of water in a 1400-ml chamber.

<sup>b</sup>Complete reaction corresponds to 491.2 ml H<sub>2</sub>/g Zr.

<sup>c</sup>Room-temperature water.

### C. Conditions for Explosive Reaction

The existence of explosive reaction rates was shown to depend on the large increase of gaseous diffusion rates when particles are in rapid motion. Rapid self-propulsion and the resulting explosive reaction rates



were found to occur with particles smaller than about 1 mm in heated water and 0.5 mm in room-temperature water. The condenser-discharge experiment with 30- and 60-mil wire specimens generates particles smaller than 1 mm when the electrical energy is sufficient to melt the specimens fully. Explosive reactions, therefore, appeared in heated water at temperatures as low as the melting point. Other experimental methods, such as the Battelle falling-drop studies,<sup>(14)</sup> did not indicate explosive reactions at temperatures near the melting point because their droplets were larger than 1 mm.

The condenser-discharge experiments in room-temperature water did not indicate explosive reactions near the melting point, presumably because the particles produced in these runs were larger than 0.5 mm in diameter. Explosive runs were encountered when the initial metal temperature was ca. 2600 C. The first oxide to form on particles at this temperature would be molten,\* and it seems likely to suppose that rapid subdivision of particles could occur under these conditions. Average particle sizes of the explosive runs were subsequently found to be lower than those of nonexplosive runs. This behavior suggests that even very large quantities of molten zirconium could rapidly subdivide, giving rise to an explosion, if the bulk of the metal reached 2600 C.

The Aerojet studies<sup>(12)</sup> provide a seeming exception to the rule that particles smaller than 0.5 mm (500  $\mu$ ) will react violently, even at temperatures as low as the metal melting point (1852 C). Although the average particle sizes of many of the explosion dynamometer runs were between 300 and 400  $\mu$ , they concluded that explosive reactions occurred when the temperature reached 2400 C. An examination of their results, however, indicates that many violent explosions (as judged by the reported values of peak pressure, pressure rise rate, total impulse, work, and overall explosion efficiency) occurred at initial metal temperatures below 2400 C. The most violent run, as judged by the efficiency, occurred at an initial metal temperature of 1950 C. The most extensive reaction of the series, 33 percent reaction, occurred with metal at 1945 C.

#### D. Discussion of Parabolic Reaction

The parabolic rate law was found to be consistent with condenser-discharge data and with 2 previous isothermal studies of the reaction rate. The parabolic rate law is usually taken as evidence that the rate-determining step of a metal-gas reaction is a solid-state diffusion process occurring within the barrier film. It is not surprising, then, that there is no sharp change in the reaction rate corresponding to the melting point of the metal. The photomicrographs shown in Figure 11 indicated that the oxide is very tenacious and survives rapid quenching to room temperature. It is, therefore, evident that the oxide shell is an effective container for the molten metal, so that there is no sharp change in the character of the reaction corresponding to metal melting.

---

\*The melting point of  $\text{ZrO}_2$  is 2700 C.

It is interesting to compare the metal-water reaction with the metal-oxygen reaction. The zirconium-oxygen reaction was reported by Porte *et al.*<sup>(32)</sup> to follow the cubic rate law between 400 and 900 C. The activation energy for the oxygen reaction was 42.7 kcal/mole, which compares closely with the value of 45.5 kcal/mole obtained for the zirconium-water reaction. The similarity suggests that the same solid-state diffusion processes are involved in both reactions. The amount of zirconium reacting with water and with oxygen in one min, 10 min, and 100 min at 1000 C are as follows:

	Reaction, mg Zr/sq cm		
	<u>1 min</u>	<u>10 min</u>	<u>100 min</u>
Zr + O <sub>2</sub>	4.0	8.6	18.6
Zr + H <sub>2</sub> O	5.6	17.6	55.6

The comparison further emphasizes the similarity of the 2 reactions. The greater tendency of zirconium to ignite in oxygen is due to the larger heat of reaction and the absence of a gaseous-diffusion barrier.

A recent study of zirconium burning in oxygen-nitrogen mixtures showed that the oxide film retained its protectiveness up to the oxide melting point of 2700 C.<sup>(33)</sup> Computed peak metal temperatures given in Tables 5 and 8 reach well above 2700 C for small particles. The accuracy of these calculations depends upon the validity of the parabolic rate law at temperatures where the oxide is molten. It seems unlikely that the rate law remains unchanged under these conditions. It is likely, however, that the molten oxide is an effective barrier to the reaction and that the reaction rate would be described by an equation very similar to the parabolic law with only moderate changes in the values of the constants. The protectiveness of molten oxide is evidenced, experimentally, by the fact that metal heated above 2700 C is not completely reacted unless the particles are very small.

#### E. Burning of Metal Vapor

Calculated peak metal temperatures for particles smaller than 520  $\mu$  in heated water reached above 3800 C, which is 200 C above the estimated normal boiling point of zirconium.<sup>(31)</sup> It seems likely that a metal vapor reaction would be involved under these extreme conditions. Calculated reaction, ignoring metal vaporization, exceeds 70 percent under these conditions, so that it makes little practical difference whether vaporization is involved or not.

It is more important to determine whether a vapor-phase ignition can occur at lower temperatures and lead to a self-sustained combustion as suggested by Epstein.<sup>(24)</sup> Epstein has suggested that an explosive reaction is initiated when the metal vapor pressure reaches 0.15 mm,

which corresponds to 2700 C for zirconium. His evidence is based on data for zirconium, uranium, aluminum, and several alkali metals. The data quoted for zirconium are the Aerojet studies, which were interpreted as showing a critical ignition temperature of 2400 C, and the studies in room-temperature water described in this report, which showed an apparent ignition temperature of 2600 C. The questionable nature of the interpretation of the Aerojet data has already been discussed. In this study, runs in heated water showed a much lower apparent ignition temperature which, moreover, was not influenced by the total pressure between values of 10 to 1500 psi. The results with heated water are just the opposite of what would be expected for a vapor-phase-initiating reaction.

Another factor which mitigates against a vapor-phase-initiating reaction below 2700 C is the strength and impermeability of the oxide coating. Metal vapor pressures of the order of a fraction of a millimeter would not be sufficient to breach the oxide shell, especially against a higher ambient pressure. The character of the residue from the reaction was not suggestive of vapor-phase burning. The oxide residue was neither highly porous nor very finely divided. Highly porous residue results from the combustion of aluminum in water.<sup>(34)</sup> The finely divided character of MgO smoke resulting from the burning of magnesium in air is well known. Both of these reactions are believed to occur by a vapor phase reaction.<sup>(34,35)</sup>

A principal argument used by Epstein in favor of vapor-phase-initiating reactions concerns the behavior of aluminum. There would seem to be no reason to believe that zirconium must behave in the same way as aluminum does. The boiling point of zirconium, ca. 3600 C,<sup>(31)</sup> is 1300 C higher than the boiling point of aluminum. Harrison<sup>(33)</sup> has shown that zirconium that burns in oxygen-enriched air does not smoke and appears to oxidize in the solid (or liquid) state at temperatures above 2700 C.

It is of interest to consider why zirconium does not burn via a vapor-phase reaction even at very high temperatures. Vapor-phase burning of liquid hydrocarbon droplets has been studied extensively. It has been determined that the rate-determining step is the rate of heat transfer from a gaseous flame zone to the liquid droplet.<sup>(36)</sup> The heat transfer rate must be sufficient to supply the heat of vaporization of the fuel in order to sustain the combustion. The temperature of the droplet approaches the boiling point corresponding to the ambient pressure. The temperature of the flame zone must then be considerably higher in order to provide a driving force for heat transfer. Liquid zirconium burning by a vapor-phase reaction would reach a temperature of about 3600 C at one atm. A temperature of the flame zone well above 4000 C would be required for sustained reaction. It seems very unlikely that such a temperature could be maintained in contact with liquid water. It is more likely that limited vaporization would result in cooling.

It is tacitly assumed by Epstein that a vapor-phase reaction would be very fast. It should be pointed out that droplet vaporization and the subsequent diffusion of fuel into the flame zone are by no means instantaneous processes. The burning of fuel droplets in air is described by the following equation<sup>(37)</sup>:

$$D_0^2 - D^2 = Ct \quad ,$$

where  $D$  is the diameter of the droplet remaining at time  $t$ ,  $D_0$  is the original droplet diameter, and  $C$  is a constant. The constant has a value of ca. 1.0 sq mm/sec for motor gasoline in 700 C air. It therefore requires one sec to consume a droplet only one mm in diameter. Such a burning rate is rather slow compared with some of the reaction rates experienced in this study.

## VII. APPLICATION TO REACTOR HAZARDS ANALYSIS\*

A detailed analysis of the role of zirconium-water reactions in a hazards analysis depends a great deal on the exact features of the particular reactor under consideration. It is necessary to state the conditions of a postulated accident before definite calculations of the extent and rate of reaction can be attempted. The research described in this report, however, should make such calculations more definite and reliable than heretofore. Postulated reactor accidents are divided into two groups: (a) those in which the zirconium in the core or cladding remains intact during the accident, and (b) those in which it is melted.

### A. Estimation of Zirconium-Water Reaction when Cladding Remains Intact

The analysis of a reactivity or a loss-of-coolant accident results in a determination of the anticipated temperature-time curve experienced by each part of the reactor. If it can be determined that the zirconium cladding will not be melted, it is possible to estimate the extent of metal-water reaction by direct integration of the rate law over the temperature-time path of the excursion. It can then be determined whether the heat generated by the metal-water reaction is sufficient to cause a revision of the original estimate of the temperature-time history of the accident. This kind of an analysis was discussed in Ref. 38. A more comprehensive study of the loss-of-coolant accident was reported by Owens *et al.*<sup>(22)</sup> In this study, the parabolic rate law deduced from the Battelle data<sup>(14)</sup> was integrated simultaneously with equations describing the residual decay heat. It was shown that a serious loss-of-coolant accident can lead to gradual self-heating and eventual melting of zirconium-clad fuel elements.

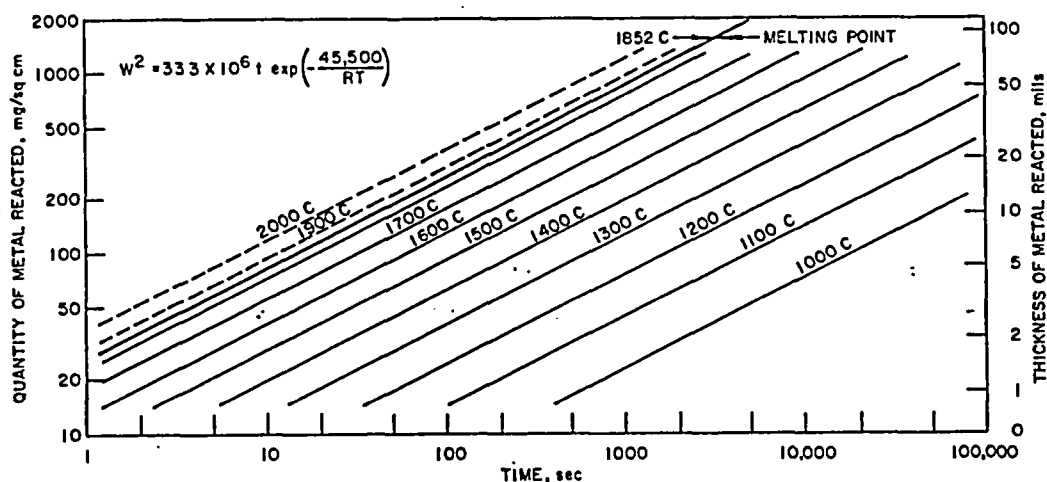
Simple estimates of the extent of reaction can be made from time at temperature considerations. This is facilitated by the solution of the rate law at a series of metal temperatures as expressed in Figure 27: A zirconium or Zircaloy tube, for example, would be expected to react to a depth of 5 mils if maintained at the melting temperature, 1852 C, for 10 sec. If the total thickness of the metal were 20 mils, this would correspond to 25% reaction. Such a simple estimate would be high because the first oxide which would form at lower temperatures, would tend to protect the surface from rapid reaction at higher temperatures. It is likely that the reaction would not be controlled by gaseous diffusion at any time under these conditions because of the slower reaction rates allowed by the parabolic rate law during the warm-up period.\*\*

---

\*This discussion is of a preliminary nature; work in this area is continuing.

\*\*This would be true in a water or a steam environment; a diffusion limitation would occur in a steam environment containing inert gas.

Figure 27  
GRAPHICAL REPRESENTATION OF PARABOLIC RATE LAW



The calculation procedures outlined above might also be valid if the reactor calculations indicated that the clad will reach temperatures only slightly above the melting point because of the high surface tension of the molten metal and the tendency of the oxide film to support and contain the molten metal. This would be true only if the clad were not subject to excessive mechanical forces during this time.

It should be emphasized that the heat of fusion cannot be neglected in any transient calculations involving zirconium. The latent heat of fusion of zirconium is equivalent to the heat needed to raise the temperature of the molten metal over 600 C. The melting temperature is located at a very strategic position in relation to reaction rates and cooling rates in transient calculations.

#### B. Estimation of Zirconium-Water Reaction when Cladding is Melted

When calculations of a postulated reactor accident indicate that the cladding will be melted, it becomes necessary to consider what particle sizes will be produced and at what point in the heating cycle the particles will separate from the bulk of the cladding. Once molten particles are formed, it should be possible to determine their fate, by means of concepts developed in the previous chapters. Molten particles formed from a partly oxidized plate or tube would very likely have a surface consisting of fresh metal. If they then enter a water environment, it is reasonable to suppose that they will react to the same extent as particles formed in the condenser-discharge experiment. The reaction experienced by each particle before cooling to the water temperature will then be given by the theoretical curves in Figure 26.

There appears to be no theoretical approach to the problem of predicting what particle sizes will be produced during a meltdown.\* It is necessary to resort to experiment. Experiments of this sort have been conducted in TREAT by Liimatainen *et al.*<sup>(2)</sup> In these studies, small fuel pins are exposed to an intense neutron burst in a water environment in TREAT. The nature of the fuel element damage, including the particle size distribution, is determined. The transient temperature and pressure and the total extent of metal-water reaction are also determined.

### 1. Comparison with TREAT Studies

The method of estimating the total extent of zirconium-water reaction developed in previous chapters was applied to 4 runs performed in the TREAT reactor. The 4 TREAT runs were made with ceramic-core, Zircaloy-2-clad fuel pins.<sup>(2)</sup> Pertinent data for the runs, including the particle size distribution, are given in Table 10.

Table 10

#### IN-PILE METAL-WATER EXPERIMENTS IN TREAT (Room-temperature water)

Core material: mixed oxide (composition, w/o: 81.5 ZrO<sub>2</sub>,  
9.1 CaO, 8.7 U<sub>3</sub>O<sub>8</sub>, 0.7 Al<sub>2</sub>O<sub>3</sub>)  
Clad material: Zr-2 (20 mils thick)  
Overall diameter: 0.38 in.  
Overall length: 1.05 in.

		CEN Transient			
		28	29	30	49
Reactor Characteristics					
Mw-sec burst		320	385	550	648
Period, msec		60	63	62	50
Energy, cal/g of oxide core		301	362	517	610
Particle Diameter - Reaction Data					
Size Group, mils	Theoretical Percent Reaction for Each Size Group <sup>a</sup>	Particle Size Distribution, <sup>b</sup> w/o			
1-4	70	0.0005	0.0002	0.1	0.03
4-8	60	0.01	0.024	1.3	0.2
8-16	46	0.2	0.10	6.5	2.8
16-32	28	2.1	3.0	2.0	15.2
32-64	14	11.2	9.7	12.8	25.2
64-128	9	22.3	27.8	77.3	57.6
128-256	6	64.3	59.4	0	0
256-512	-	0	0	0	0
Percent of Metal Reacted with Water					
Calculated		8.1	8.3	13.1	14.4
Experimental		4.1	8.0	14.0	24.0

<sup>a</sup>Data taken from Figure 26

<sup>b</sup>Particle size distribution for total sample (metal and oxide).

\* L. F. Epstein has also reached this conclusion.<sup>(21)</sup>

The estimated extent of reaction for each particle size group was obtained from analog computer results for runs in room-temperature water (given by the lower solid curve in Figure 26) and is given in the table. The anticipated reaction of each particle size group was then summed to give an estimate of the overall extent of reaction. The calculated values are compared in the table with experimental values obtained by a determination of the hydrogen generated by the reaction. The calculated values and the experimental values agree accurately for 2 of the runs, but deviate for the highest and lowest energy runs.

The amount of reaction occurring before the cladding was melted was ignored in this calculation. It is likely that the fuel pin temperature went from 1000 C, at which significant reaction might begin, to a fully melted state in less than 0.2 sec.\* This would result in an oxide layer thickness of a fraction of a mil, which would correspond to only one or two percent metal-water reaction, since the original cladding was 20 mils in thickness. It is likely that reaction occurring before melting can be ignored in fast transients where there is extensive particle formation and considerable reaction.

Some of the particles formed in the TREAT runs were in the size range that would be predicted to be explosive on the basis of the laboratory data. No explosive pressure rises, however, were observed in the TREAT runs referred to in Table 10. This suggests that the particles were formed over a period of time so that, although each particle smaller than 0.5 mm (19.7 mils) would be rapidly consumed, the overall reaction would be relatively slow. An estimate of the reaction rate could be obtained if it were assumed that the rate of formation of particles was identical to the rate of metal melting.

## 2. Reactions with Uranium-Zirconium Alloys

Discussions have thus far been limited to zirconium and Zircaloy alloys. Uranium-zirconium alloy fuels constitute a fundamentally different case for 2 reasons. First, it is likely that the constants of the rate law are different for these alloys because of the greater reactivity of uranium. It might be assumed, as a first approximation, that the rate law found for pure zirconium applies to zirconium-rich alloys. The reaction rate of zirconium with oxygen was increased only slightly when up to 3.5 a/o uranium was alloyed with the zirconium.<sup>(32)</sup> The reaction, however, experienced a breakaway to a more rapid linear reaction after ca. 7.5 mg Zr/sq cm reaction at 700 C. The rate of post-breakaway reaction was 0.005 mg Zr/(sq cm)(min).

---

\*Heating rates were estimated to be about 8000 C/sec in these studies.



The second important difference between accident calculations for zirconium compared with those for zirconium-uranium alloys is the fact that uranium-bearing particles continue to be heated by the neutron field after separating from the fuel element. Calculation of the fate of such particles requires the insertion of an additional heat-generation term in Equations 25 and 26, Chapter IV. This term would include an expression for the transient value of the neutron flux and the uranium enrichment, and clearly would be specific for a particular accident situation. Methods for including the fission heating term in metal-water reaction calculations were discussed by Liimatainen *et al.*<sup>(39)</sup> These studies are continuing in connection with TREAT meltdown studies.

### 3. Effect of Water Temperature and Total Pressure

The quantitative methods used to formulate the effect of water temperature and inert gas pressure on rates of gaseous diffusion were semi-empirical. Heat transfer and diffusion effects in subcooled liquids are not well understood,\* and no simple relationships existed which could be applied to the case at hand. Experimentally, there were found to be 2 distinct cases. Slower rates occurred in room-temperature water with or without one atm. of inert gas. Faster rates occurred when the water temperature was between 90 and 315 C with or without 2 atm of inert gas. Agreement between calculated and experimental results was obtained in the case of heated water when the water vapor pressure, driving diffusion, was set equal to the total pressure ( $\Delta P_w/P = 1$ ). Agreement was obtained in the room-temperature case when the ratio  $\Delta P_w/P$  was set equal to 0.5. The latter was taken to mean, physically, that about one-half of the water at the water-water vapor interface, adjacent to reacting particles, reached the boiling point while one-half remained at the bulk water temperature. These assumptions were sufficient to explain the results of this study. It is of interest to extend these assumptions to cases not studied experimentally, even though the conclusions must be considered speculative.

The assumption can be expressed as follows:

$$\text{Diffusion Rate} \propto \frac{0.5 (\text{Vapor Pressure}) + 0.5 (\text{Total Pressure})}{\text{Total Pressure}}$$

The predicted ratios for a number of cases are calculated in Table 11. Cases which would appear to have values intermediate between 0.5 and 1.0 were best described by the heated water calculation ( $\Delta P_w/P = 1$ ). It would therefore be logical to consider molten zirconium in an operating PWR to have the maximum possible diffusional reaction rate. A BWR would be subject to the more rapid rates of gaseous diffusion throughout most of the startup period, as well as during operation.

---

\*It should be noted here that the very large heat transfer coefficients usually associated with subcooled boiling<sup>(40)</sup> are not realized when a metal-water reaction is in progress. Hydrogen generated by reaction stabilizes a thick boundary film, preventing the formation of the very thin and violently agitated film that is characteristic of metal quenching in cold water.

Table 11

ESTIMATION OF RELATIVE RATES OF GASEOUS DIFFUSION FOR  
VARIOUS WATER TEMPERATURES AND TOTAL PRESSURES

Water Temp, C	Saturated Vapor Pressure, psi	Total Pressure, psi	Relative Rate of Gaseous Diffusion	Equivalent Case
This Study				
25	0.5	5	0.55	Room-temp Water Run, after 7% Reaction
		25	0.51	Room-temp Water Run, after 35% Reaction
		15	0.52	Room-temp Water Run, with Added Argon
100	15	20	0.88	Heated-water Run, after 7% Reaction
		40	0.69	Heated-water Run, after 35% Reaction
		30	0.75	Heated-water Run, with Added Argon
315	1500	1500	1.00	Heated-water Run, at Highest Pressure
Typical Boiling Water Reactor				
25	0.5	5	0.55	Cold Reactor, Partial Vacuum
100	15	15	1.00	During Warm-up
283	1000	1000	1.00	Operating
Typical Pressurized Water Reactor				
25	0.5	15	0.52	Cold Reactor
100	15	2000	0.50	During Warm-up
283	1000	2000	0.75	Operating

The most uncertain case is the PWR during warm-up, during which a very large total pressure is applied while the water is still relatively cool. The possibility exists that the relative diffusional rate might be lower than 0.50. The data of Milich and King (see Table 9) would tend to make this unlikely. Their results indicated that large pressures of inert gas were no more effective in suppressing reaction than was one atm of inert gas. Their results constitute important verification of the simple formula given for diffusion rate.

## VIII. REFERENCES

1. L. Baker, Jr., R. L. Warchal, R. C. Vogel, and M. Kilpatrick, Studies of Metal-Water Reactions at High Temperatures: I. The Condenser-discharge Experiment: Preliminary Results with Zirconium, ANL-6257 (May 1961).
2. R. C. Liimatainen, R. O. Ivins, M. F. Deerwester, and F. J. Testa, Studies of Metal-Water Reactions at High Temperatures: II. TREAT Experiments, Status Report on Results with Aluminum, Stainless Steel-304, Uranium, and Zircaloy-2, ANL-6250 (Jan 1962).
3. W. C. Ruebsamen, F. J. Shon, and J. B. Chrisney, Chemical Reaction between Water and Rapidly Heated Metals, NAA-SR-197 (Oct 1952).
4. W. A. Bostrom, The High Temperature Oxidation of Zircaloy in Water, WAPD-104 (March 1954).
5. B. Lustman, Zirconium-Water Reactions, WAPD-137 (Dec 1955).
6. W. Milich and E. C. King, Molten Metal-Water Reactions, NP-5813, Tech. Rpt. No. 44 (Nov 1955).
7. W. N. Lorentz, Chemical Reaction of Zirconium-Uranium Alloys in Water at High Temperatures, WAPD-PM-22 (del.) (July 1955).
8. O. J. Elgert and A. W. Brown, In-pile Molten Metal-Water Reaction Experiments, IDO-16257 (June 1956).
9. D. C. Layman and H. L. Mars, Some Qualitative Observations of the Zirconium-Water Reaction at Atmospheric Pressure, KAPL-1534 (April 1956).
10. H. M. Higgins, A Study of the Reaction of Metals and Water, AECD-3664 (April 1955).
11. H. M. Higgins, The Reaction of Molten Uranium and Zirconium, AGC-AE-17 (April 1956).
12. H. M. Higgins and R. D. Schultz, The Reaction of Metals in Oxidizing Gases at High Temperatures, IDO-28000 (April 1957).
13. H. M. Saltsburg, Metal-Water Reactions, KAPL-1495 (April 1956).
14. A. W. Lemmon, Jr., Studies Relating to the Reaction between Zirconium and Water at High Temperatures, BMI-1154 (Jan 1957).

15. E. Janssen, W. H. Cook, and K. Hikido, Metal-Water Reactions: I. A Method for Analyzing a Nuclear Excursion in a Water-cooled and Moderated Reactor, GEAP-3073 (Oct 1958).
16. J. I. Owens, Metal-Water Reactions: II. An Evaluation of Severe Nuclear Excursions in Light Water Reactors, GEAP-3178 (June 1959).
17. K. M. Horst, Metal-Water Reactions: III. Fuel Element Stresses during a Nuclear Accident, GEAP-3191 (July 1959).
18. K. Hikido, Metal-Water Reactions: IV. Heat Transfer Conditions during Severe Nuclear Excursions in Water Cooled Reactors, GEAP-3204 (Sept 1959).
19. S. C. Furman, Metal-Water Reactions: V. The Kinetics of Metal-Water Reactions - Low Pressure Studies, GEAP-3208 (July 1959).
20. L. F. Epstein, Metal-Water Reactions: VI. Analytical Formulations for the Reaction Rate, GEAP-3272 (Sept 1959).
21. L. F. Epstein, Metal-Water Reactions: VII. Reactor Safety Aspects of Metal-Water Reactions, GEAP-3335 (Jan 1960).
22. J. I. Owens, R. W. Lockhart, D. R. Iltis, and K. Hikido, Metal-Water Reactions: VIII. Preliminary Consideration of the Effects of a Zircaloy-Water Reaction during a Loss of Coolant Accident in a Nuclear Reactor, GEAP-3279 (Sept 1959).
23. S. C. Furman and P. A. McManus, Metal-Water Reactions: IX. The Kinetics of Metal-Water Reactions - Feasibility Study of Some New Techniques, GEAP-3338 (Jan 1960).
24. L. F. Epstein, Correlation and Prediction of Explosive Metal-Water Reaction Temperatures, Nucl. Sci. and Engr. 10, 247 (1961).
25. J. W. Westwater, "Boiling of Liquids" in Advances in Chemical Engineering, Academic Press Inc., N. Y., (1956), Vol. I, p. 1 ff.
26. E. R. G. Eckert, Introduction to the Transfer of Heat and Mass, McGraw-Hill Book Co. (1950), p. 251 ff.
27. D. A. Frank-Kamenetskii, Diffusion and Heat Exchange in Chemical Kinetics, Princeton University Press, Princeton, N. J. (1955).
28. O. Kubaschewski and B. E. Hopkins, Oxidation of Metals and Alloys, Butterworths Scientific Publications, London (1953).

29. J. O. Hirschfelder, C. F. Curtiss, and R. B. Bird, Molecular Theory of Gases and Liquids, John Wiley and Sons, Inc.; New York (1954).
30. V. N. Huff, S. Gordon, and V. E. Morrell, General Method and Thermodynamic Tables For Computation of Equilibrium Composition and Temperature of Chemical Reactions, NACA Report 1037 (1951).
31. A. Glassner, The Thermochemical Properties of the Oxides, Fluorides, and Chlorides to 2500 K, ANL-5750 (1957).
32. H. A. Porte, J. G. Schnizlein, R. C. Vogel, and D. F. Fischer, Oxidation of Zirconium and Zirconium Alloys, ANL-6046 (Sept 1959).
33. P. L. Harrison and A. D. Yoffe, The Burning of Metals, Proc. Roy. Soc. (London) A261, 357 (1961).
34. R. E. Wilson, unpublished work, ANL.
35. K. P. Coffin, Some Physical Aspects of the Combustion of Magnesium Ribbons, "Fifth Symposium (International) on Combustion," Reinhold Corp., New York (1955), p. 267.
36. H. Wise, J. Lorell, and B. J. Wood, The Effects of Chemical and Physical Parameters on the Burning Rate of a Liquid Droplet, "Fifth Symposium (International) on Combustion," Reinhold Corp., New York (1955), p. 132.
37. K. Kobayasi, An Experimental Study on the Combustion of a Fuel Droplet, "Fifth Symposium (International) on Combustion," Reinhold Corp., New York (1955), p. 141.
38. Power Reactor Technology, A Quarterly Technical Progress Review, 3, 1 (1959).
39. R. C. Liimatainen, H. T. Bates, L. C. Just and N. F. Morehouse, Jr., Analog Computer Study of Metal-Water Reactions Initiated by Nuclear Reactor Transients, ANL-6129 (May 1960).
40. J. W. Westwater, "Boiling of Liquids" in Advances in Chemical Engineering, Academic Press Inc., New York (1958) Vol. II, p. 21.
41. R. E. Carter, A Kinetic Model for Solid-state Reactions, General Electric Research Laboratory Report No. 60-RL-2589 M (Dec 1960).
42. G. P. Harnwell, Principles of Electricity and Electromagnetism, 2nd Ed., McGraw-Hill Book Co., New York (1949), p. 102.

## IX. ACKNOWLEDGMENTS

Thanks are due to R. C. Vogel of the Chemical Engineering Division, M. Kilpatrick of the Chemistry Division, and N. F. Morehouse, Jr., of the Applied Mathematics Division for their guidance and encouragement throughout this program. The authors wish to thank R. Liimatainen and R. O. Ivins of the Chemical Engineering Division for many useful discussions. The authors are indebted to C. H. Bean and the Metallurgy Division of ANL for preparation of the zirconium wires, and to R. L. Warchal of the Chemical Engineering Division who performed the condenser-discharge experiments. We also acknowledge the assistance of D. Anthes, M. Deerwester, F. Testa, and L. Mishler for preparing photomicrographs, R. Koonz and T. Kato who assisted in the particle size determinations, and M. Homa and R. Schablaske who performed the X-ray diffraction studies.



## X. APPENDICES

### Appendix A

#### EXPERIMENTAL DATA TABLES

Numerical results of the condenser-discharge studies of the zirconium-water reaction are given in Tables A1 through A4. The energy input is the electrical energy given to the specimen wires by the discharging condensers. Metal temperatures were calculated on the basis that the energy addition occurred adiabatically. The vapor pressure of water was measured in some cases and obtained from measurements of water temperature in others. The percent reaction was calculated from a determination of the quantity of hydrogen generated by the reaction, assuming that zirconium dioxide ( $\text{ZrO}_2$ ) was the only solid product formed and that no hydrogen was retained by the residue. Sauter mean particle diameters were measured by an optical method. Equivalent particle diameters are given for those specimens which remained intact or were in the form of a distorted wire. The equivalent particle sizes are the diameters of spheres that would have the same surface-to-volume ratio as the original wire.



Table A1

## RUNS WITH 60-MIL ZIRCONIUM WIRES IN ROOM-TEMPERATURE WATER

Run	Energy Input, cal/g	Calc Metal Temp, C, and Physical State	Pressure of Added Argon, psi	Percent Reaction	Mean Particle Diameter, $\mu$	Appearance of Residue
I. No Inert Gas; Vapor Volume 40 cc						
32	100	1100, Solid	-	0.7	2140	Intact
23	127	1500, Solid	-	1.2	2180	Intact
13	137	1600, Solid	-	3.9	2160	Intact
192	144	1700, Solid	-	2.6	2300	Intact
22	150	1800, Solid	-	4.2	2170	Intact
193	157	1852, Solid	-	3.7	2300	Intact
24	158	1852, 10% Liquid	-	5.9	2060	Distorted Wire
28	174	1852, 30% Liquid	-	-	2180	Distorted Wire
27	183	1852, 50% Liquid	-	-	2240	Distorted Wire
202	185	1852, 50% Liquid	-	11.3	- <sup>a</sup>	Spherical Particles
226	189	1852, 60% Liquid	-	9.9	- <sup>a</sup>	Distorted Wire
25	190	1852, 60% Liquid	-	8.9	2280	Spherical Particles
52	198	1852, 70% Liquid	-	10.2	1740	Spherical Particles
197	201	1852, 80% Liquid	-	11.2	- <sup>a</sup>	Spherical Particles
26	203	1852, 80% Liquid	-	7.9	2100	Spherical Particles
29	209	1852, 90% Liquid	-	7.9	1500	Spherical Particles
14	217	1900, Liquid	-	8.2	1960	Distorted Wire
15	218	1900, Liquid	-	9.0	2040	Spherical Particles
18	233	2100, Liquid	-	12.1	1500	Spherical Particles
30	235	2100, Liquid	-	12.6	940	Spherical Particles
228	236	2100, Liquid	-	14.0	- <sup>a</sup>	Spherical Particles
31	258	2400, Liquid	-	18.3	680	Spherical Particles
42	269	2500, Liquid	-	10.9	740	Spherical Particles
20	275	2600, Liquid <sup>b</sup>	-	24.0	440	Spherical Particles
19	276	2600, Liquid <sup>b</sup>	-	43.0	340	Spherical Particles
16	284	2700, Liquid	-	17.1	980	Spherical Particles
40	290	2800, Liquid <sup>b</sup>	-	39.0	160	Spherical Particles
41	294	2800, Liquid <sup>b</sup>	-	71.0	110	Spherical Particles
17	296	2900, Liquid <sup>b</sup>	-	45.0	340	Spherical Particles
39	300	2900, Liquid <sup>b</sup>	-	50.0	240	Spherical Particles
21	313	3100, Liquid <sup>b</sup>	-	37.0	240	Spherical Particles
53	322	3200, Liquid <sup>b</sup>	-	51.0	370	Spherical Particles
37	332	3300, Liquid <sup>b</sup>	-	52.0	180	Spherical Particles
35	361	3700, Liquid <sup>b</sup>	-	60.0	200	Spherical Particles
34	388	4100, Liquid <sup>b</sup>	-	71.0	270	Spherical Particles
36	393	4100, Liquid <sup>b</sup>	-	50.0	480	Spherical Particles
II. No Inert Gas; Vapor Volume 160 cc						
237	142	1700	-	5.1	- <sup>a</sup>	Intact
235	158	1852, 10% Liquid	-	10.5	- <sup>a</sup>	Distorted Wire
238	159	1852, 10% Liquid	-	5.8	- <sup>a</sup>	Distorted Wire
239	195	1852, 70% Liquid	-	12.8	- <sup>a</sup>	Distorted Wire
232	204	1852, 80% Liquid	-	13.2	- <sup>a</sup>	Spherical Particles
231	226	2000, Liquid	-	13.2	- <sup>a</sup>	Spherical Particles
III. Added Argon Gas; Vapor Volume 40 cc						
241	168	1852, 20% Liquid	15	4.5	- <sup>a</sup>	Distorted Wire
240	174	1852, 30% Liquid	15	4.2	- <sup>a</sup>	Distorted Wire
205	195	1852, 70% Liquid	20	7.7	- <sup>a</sup>	Flattened Pieces
204	195	1852, 70% Liquid	25	8.9	- <sup>a</sup>	Flattened Pieces
243	213	1852, 100% Liquid	15	7.9	- <sup>a</sup>	Spherical Particles

<sup>a</sup>Mean particle diameter not determined<sup>b</sup>Runs had an explosive pressure rise

Table A2

## RUNS WITH 30-MIL ZIRCONIUM WIRES IN ROOM TEMPERATURE WATER

Run	Input Energy, cal/g	Calc Metal Temp, C, and Physical State	Percent Reaction	Mean Particle Diameter, $\mu$	Appearance of Residue
85	124	1500, Solid	5.9	1120	Intact
86	146	1700, Solid	10.0	1130	Two Pieces
71	149	1800, Solid	8.6	1160	Four Pieces
88	160	1852, 10% Liquid	13.7	1100	Distorted Wire
89	163	1852, 10% Liquid	12.3	1010	Distorted Wire
87	165	1852, 20% Liquid	15.6	1010	Distorted Wire
75	180	1852, 40% Liquid	12.6	1040	Distorted Wire
76	182	1852, 40% Liquid	16.4	1040	Distorted Wire
72	190	1852, 60% Liquid	11.8	1630	Spherical Particles
107	198	1852, 70% Liquid	13.8	1390	Spherical Particles
82	214	1852, 100% Liquid	18.5	1200	Spherical Particles
90	214	1852, 100% Liquid	19.7	1290	Spherical Particles
108	231	2100, Liquid	14.8	1680	Spherical Particles
106	232	2100, Liquid	18.1	1020	Spherical Particles
83	241	2200, Liquid	14.8	1180	Spherical Particles
112	255	2400, Liquid	15.3	1610	Spherical Particles
74	270	2500, Liquid	23.9	780	Spherical Particles
109	290	2800, Liquid <sup>a</sup>	43.8	300	Spherical Particles
111	296	2900, Liquid <sup>a</sup>	22.6	650	Spherical Particles
110	314	3100, Liquid <sup>a</sup>	45.7	320	Spherical Particles
73	324	3200, Liquid <sup>a</sup>	44.9	330	Spherical Particles
113	387	4000, Liquid <sup>a</sup>	38.0	420	Spherical Particles
114	482	- , Part Vapor <sup>a</sup>	49.7	440	Spherical Particles

<sup>a</sup>Runs had an explosive pressure rise.

Table A3

## RUNS WITH 60-MIL ZIRCONIUM WIRES IN HEATED WATER

Run	Energy Input, cal/g	Calc Metal Temp, C, and Physical State	Water Vapor Pressure, psi	Pressure of Added Argon, psi	Percent Reaction	Mean Particle Diameter, $\mu$	Appearance of Residue
I. Water Temperature 90-125 C; No Inert Gas							
194	150	1852, Solid	10	-	8.6	2390	Distorted Wire
191	150	1852, Solid	32	-	7.8	2300	Distorted Wire
196	204	1852, 90% Liquid	22	-	31.5	1260	Spherical Particles
200	216	1900, Liquid	19	-	51.7	1320	Spherical Particles
223	219	2000, Liquid <sup>a</sup>	22	-	55.5	690	Spherical Particles
225	221	2000, Liquid <sup>a</sup>	28	-	51.3	650	Spherical Particles
217	244	2300, Liquid <sup>a</sup>	19	-	90.3	495	Spherical Particles
219	271	2600, Liquid <sup>a</sup>	16	-	82.9	480	Spherical Particles
222	309	3100, Liquid <sup>a</sup>	19	-	81.0	670	Spherical Particles
II. Water Temperature 140-200 C; No Inert Gas							
195	157	1852, 30% Liquid	215	-	9.0	2300	Distorted Wire
190	161	1852, 30% Liquid	225	-	8.5	2300	Distorted Wire
189	169	1852, 40% Liquid	205	-	14.5	1500	Spherical Particles
203	203	1852, 100% Liquid <sup>a</sup>	50	-	55.2	670	Spherical Particles
188	206	1900, Liquid <sup>b</sup>	155	-	30.7	800	Spherical Particles
227	230	2200, Liquid <sup>a</sup>	88	-	55.1	650	Spherical Particles
218	252	2500, Liquid <sup>a</sup>	79	-	52.0	1150	Spherical Particles
220	277	2800, Liquid <sup>a</sup>	150	-	73.8	420	Spherical Particles
III. Water Temperature 280-315 C; No Inert Gas							
216	151	1852, 30% Liquid	1500	-	11.4	2300	Distorted Wire
234	186	1852, 90% Liquid	1500	-	25.9	630	Spherical Particles
213	194	1852, 100% Liquid <sup>b</sup>	900	-	25.9	700	Spherical Particles
233	205	2000, Liquid <sup>b</sup>	1500	-	30.0	1370	Spherical Particles
230	215	2100, Liquid <sup>a</sup>	1500	-	49.1	730	Spherical Particles
229	232	2400, Liquid <sup>a</sup>	1500	-	54.6	520	Spherical Particles
IV. Added Argon Gas							
279	148	1852, Solid	16	20	7.9	-	Three Pieces
206	205	1852, 90% Liquid <sup>a</sup>	26	20	37.6	830	Spherical Particles
278	215	1900, Liquid <sup>a</sup>	17	20	78.8	-	Powder
280	232	2200, Liquid <sup>a</sup>	18	20	85.2	-	Powder

<sup>a</sup>Runs had an explosive pressure rise.<sup>b</sup>No pressure trace obtained.

Table A4  
RUNS WITH 60-MIL ZIRCALOY-3 WIRES

Run	Energy Input, cal/g	Calc Metal Temp, C, and Physical State	Water Vapor Pressure, psi	Percent Reaction	Appearance of Residue
I. Room Temperature Water					
273	165	1852, 20% Liquid	0.5	6.3	Distorted Wire
274	206	1852, 80% Liquid	0.5	10.9	Spherical Particles
275	251	2300, Liquid <sup>b</sup>	0.5	16.7	Spherical Particles
276	298	2900, Liquid <sup>a</sup>	0.5	27.0	Spherical Particles
277	314	3100, Liquid <sup>a</sup>	0.5	58.4	Spherical Particles
II. Heated Water 105-115 C					
267	141	1700, Solid	23	7.5	Intact
268	219	2000, Liquid <sup>a</sup>	21	40.2	Spherical Particles
269	240	2200, Liquid <sup>a</sup>	21	58.2	Spherical Particles
270	299	3000, Liquid <sup>a</sup>	19	93.1	Spherical Particles
271	340	3500, Liquid <sup>a</sup>	18	83.4	Spherical Particles
272	370	3900, Liquid <sup>a</sup>	18	79.4	Spherical Particles

<sup>a</sup>Runs had an explosive pressure rise.

<sup>b</sup>No pressure trace obtained.

## Appendix B

EFFECT OF NON-PLANAR GEOMETRY ON  
THE PARABOLIC RATE LAW

The parabolic rate law, expressed in the differential form as follows,

$$\frac{d(x_0 - x)}{dt} \propto \frac{1}{x_0 - x} \quad (\text{B1})$$

is rigorously correct only for a solid-state diffusion process occurring at a plane surface. Diffusion through a barrier film on a cylindrical or spherical surface must depend not only on the thickness of the barrier,  $x_0 - x$  but also on the ratio of the inner radius  $x$  to the outer radius  $x_0$ . This was pointed out by Epstein in Ref. 20 and by Carter in Ref. 41. Epstein derived the correct form of the parabolic rate law for cylindrical and spherical geometry by a detailed solution of Fick's law of diffusion. Carter derived the identical relation for spherical geometry by equating the steady-state equation for diffusion through a spherical shell to the instantaneous reaction rate. Carter's equation also provided for the difference in density between the metal and the oxide.

The equations will be derived here by a simple analogy to the flow of electric current. Solid-state diffusion through an insulating crystal can, in fact, be considered as a current of ions migrating under the influence of an emf.<sup>(28)</sup> The reaction rate can be identified with the current, and Ohm's law may be formally applied as follows:

$$\text{Reaction rate} \propto \text{emf/Resistance} \quad (\text{B2})$$

The electrical resistance is expressed in terms of resistivity for 3 cases as follows:<sup>(42)</sup>

$$\text{Plane} \quad \text{Resistance} = \text{Resistivity} \left( \frac{x_0 - x}{A} \right) \quad (\text{B3a})$$

$$\text{Cylindrical Shell} \quad \text{Resistance} = \text{Resistivity} \left( \frac{\ln[x_0/x]}{2\pi L} \right) \quad (\text{B3b})$$

$$\text{Spherical Shell} \quad \text{Resistance} = \text{Resistivity} \left( \frac{x_0 - x}{4\pi x x_0} \right) \quad (\text{B3c})$$

where  $A$  is the planar area normal to current flow, and  $L$  is the length of the cylinder. The volumetric reaction rate (cc metal/sec) can be expressed as follows for the 3 cases:

$$\text{Plane:} \quad \text{Reaction rate} = A \frac{d(x_0 - x)}{dt} \quad (\text{B4a})$$

$$\text{Cylinder:} \quad \text{Reaction rate} = 2\pi Lx \frac{d(x_0 - x)}{dt} \quad (\text{B4b})$$

$$\text{Sphere:} \quad \text{Reaction rate} = 4\pi x^2 \frac{d(x_0 - x)}{dt} \quad (\text{B4c})$$

Substituting Equations B3 into B2 and equating Equation B2 to Equations B4 yield the following:

$$\text{Plane:} \quad \frac{d(x_0 - x)}{dt} \propto \frac{1}{x_0 - x} \quad (\text{B5a})$$

$$\text{Cylinder:} \quad \frac{d(x_0 - x)}{dt} \propto \frac{1}{x \ln(x_0/x)} \quad (\text{B5b})$$

$$\text{Sphere:} \quad \frac{d(x_0 - x)}{dt} \propto \frac{x_0}{x(x_0 - x)} \quad (\text{B5c})$$

Equation B5a is identical with Equation B1 and represents the parabolic rate law for a plane surface. Equations B5b and B5c represent the parabolic law for a cylindrical and a spherical surface, respectively. The integrated forms of the rate laws are obtained by integrating Equations B5 as follows:

$$\text{Plane:} \quad (x_0 - x)^2 \propto t \quad (\text{B6a})$$

$$\text{Cylinder:} \quad x^2 \ln\left(\frac{x}{x_0}\right) + \frac{x_0^2 - x^2}{2} \propto t \quad (\text{B6b})$$

Expanding the logarithmic term and simplifying yields

$$(x_0 - x)^2 \left[ 1 - 1/3 \left( \frac{x_0 - x}{x_0} \right) - 1/12 \left( \frac{x_0 - x}{x_0} \right)^2 - \dots \right] \propto t$$

Sphere:

$$(x_0 - x)^2 \left[ 1 - 2/3 \left( \frac{x_0 - x}{x_0} \right) \right] \propto t \quad (\text{B6c})$$

The error introduced by applying the simplified rate law Equation B5a to spheres is found by comparing Equation B5a with Equation B5c. The correct rate for the spherical case is seen to be greater than the approximate value by a factor of  $x_0/x$ . The following table gives numerical values for the ratio of the rates.

<u>Percent of Sphere Reacted <math>100 [1-(x/x_0)^3]</math></u>	<u>True Rate/Approximate Rate</u>
0	1.000
10	1.035
25	1.10
50	1.26
75	1.59

## Appendix C

## ANALOG COMPUTER INFORMATION

A. General Information

The analog computer used in this study was an Electronic Associates PACE, model 131 R. The analog model of the metal-water reactions involves standard techniques with possibly one exception, a relay circuit to control the model during phase changes.

For complete information about the analog computer installation at Argonne, see ANL-6075; for information about the programming of an analog computer, see ANL-6187.

B. Programming Information

## 1. Equations

$$\left(\frac{dx}{dt}\right)_k^* = -\frac{B}{x_0 - x} \exp(-G/T_s) \quad : \quad \text{Parabolic Rate}$$

$$\left(\frac{dx}{dt}\right)_d = Kx_0 \frac{(T_s + T_w)^{0.68}}{x^2} \frac{\Delta P_w}{P} \quad : \quad \text{Diffusion Rate}$$

$$\frac{\Delta P_w}{P} = \text{constant or a function of \% of reaction}$$

$$\frac{dx}{dt} = \text{Minimum} \{\dot{x}_k, \dot{x}_d\}$$

$$\frac{dT_m}{dt} = \frac{1}{w} \left[ -\frac{N}{x_0^3} x^2 \frac{dx}{dt} - \frac{y}{x_0} (T_s^4 - T_w^4) - \frac{U}{x_0^2} (T_s + T_w)^{0.88} (T_s - T_w) \right]$$

$$\frac{dF}{dt} = \frac{M}{L'} \frac{dT_m}{dt} \quad ; \quad \text{used during freezing and melting}$$

$$T_s = T_m + \frac{(x_0 - x)x_0^3}{P x_0 x} \left[ -\frac{y}{x_0} (T_s^4 - T_w^4) - \frac{U}{x_0^2} (T_s + T_w)^{0.88} (T_s - T_w) \right]$$

---

\*The division by zero that appears has no effect on the equations since  $\dot{x}_d > \dot{x}_k$  at  $x = x_0$



## Initial Conditions

$$x = x_0$$

$$T_m = T_s > 300^\circ\text{K}$$

2. Machine Variables and Scale Factors

$$t' = at \quad ; \quad a > 1$$

$$x' = bx \quad ; \quad b > 1$$

$$T' = cT \quad ; \quad c < 1$$

$$F' = mF \quad ; \quad m > 1$$

The variable  $x$  represents particle radius and was one of the parameters in the investigation. As  $x_0$  is changed,  $b$  will be changed so that  $bx_0$  is constant. For  $x_0 = 0.105$  cm,  $b = 500$ , so  $x'_0 = 52.50$  v. For  $x_0 = 0.0525$  cm,  $b = 1000$ .

These reactions speed up as  $x(0)$  is made smaller. Therefore  $a = 10^2$  for  $x_0 = 0.105$  or  $0.0525$  cm;  $10^3$  for  $x_0 = 0.026$  or  $0.013$ ; and  $a = 10^4$  for  $x_0 = 0.006$  cm.

$$c = 10^{-2}, \text{ so that } T < 10,000^\circ\text{K}.$$

$$m = 100 \text{ so that } 1 \text{ volt represents } 1\% \text{ melted metal.}$$

3. Scaled Equations

$$\left(\frac{dx'}{dt}\right)_k = -\frac{B b^2}{a} \frac{\exp(-c G_2/T'_s)}{x'_0 - x'}$$

$$\left(\frac{dx'}{dt}\right)_D = \frac{b^3 x_0 K}{a c^{0.68}} \frac{(T'_s + T'_w)^{0.68}}{x'^2} \frac{\Delta P_w}{P}$$

$$\frac{dx'}{dt'} = \text{Minimum} \{ \bar{x}'_0, \bar{x}'_k \}$$

$$\frac{dT'_m}{dt'} = \frac{10^2 c}{M} [I + II + III + IV]$$

where

$$I = \frac{-N x'^2}{b^3 x_0^3 10^2} \frac{dx'}{dt'}$$

$$II = \frac{B}{a 10^2} f(t')$$

$$III = \frac{40,000 y}{ac^4 x_0 10^2} \left( \frac{T'_s - T'_w}{40,000} \right)$$

$$IV = \frac{-10 U}{10^2 a x_0^2 c^{1.88}} \left[ \frac{(T'_s + T'_w)^{0.88} (T'_s - T'_w)}{10} \right]$$

$$\frac{dF'}{dt'} = \frac{mM}{L'c} \frac{dT'}{dt'}$$

$$T'_s = T'_m + \frac{10^2 c x_0^2 a}{z} \left( \frac{x'_0 - x'}{x'} \right) (III + IV)$$

#### 4. Quantities to be Generated

In this section,  $\boxed{10^2}$  is caused by the divide circuit and  $\textcircled{10^2}$  is caused by the multiplier circuit. Fractions are not reduced to lowest terms in order that all considerations are easily seen.

$$(a) 10^2 \left( \frac{dx'}{dt'} \right)_k = - \frac{B b^2}{a 10^6} \left[ \frac{10^6 \exp(-c G/T'_s)}{x'_0 - x'} \right] \boxed{10^2}$$

$$(b) 10^2 \left( \frac{dx'}{dt'} \right)_d = - \frac{b^3 x_0 K}{a c^{0.68} 10^2} \left[ \frac{(T'_s + T'_w)^{0.68}}{\frac{x'^2}{10^2}} \right] \boxed{10^2} \frac{\Delta P_w}{P}$$

$$(c) I = - \frac{N}{x_0^3} \left( \frac{x'^2}{10^2} \right) \left( 10^2 \frac{dx'}{dt'} \right) \textcircled{10^2}$$

$$(d) II = \frac{B}{10^2 a} f(t')$$

$$(e) \text{ III} = \frac{4 y 10^4}{a c^4 x_0 10^2} \left( \frac{T_s^{14} - T_w^{14}}{4 x 10^4} \right)$$

$$(f) \text{ IV} = \frac{10 U}{10^2 a x_0^2 c^{1.88}} \left[ \frac{(T_s' + T_w')^{0.88} (T_s' - T_w')}{10} \right]$$

$$(g) \text{ I} + \text{II} + \text{III} + \text{IV}$$

$$(h) 10 (\text{III} + \text{IV})$$

$$(i) V = \frac{10^2}{10^2} \left( \frac{x_0' - x'}{x'} \right) (10 \text{ III} + 10 \text{ IV}) \left( \frac{10^2 c x_0^2 a}{10 P} \right)$$

$$(j) 100 (\% \text{ reaction}) = 10^2 - \left( \frac{10^6}{x_0^{13}} \right) \frac{x^{13}}{10^4}$$

$$(k) \left( \frac{T_s^{14} - T_w^{14}}{40,000} \right)$$

(l) A relay circuit must be provided to control the equations during melting.

Function generating equipment will be used to generate:

$$(m) (T_s' + 3)^{0.68}$$

$$(n) \frac{(T_s' + 3)^{0.88} (T_s' - 3)}{10}$$

$$(o) 10^6 \exp (-276.8/T_s')$$

$$(p) \frac{\Delta P_w}{P}$$

### 5. Potentiometer Settings

- |                                    |                     |
|------------------------------------|---------------------|
| 1. $0.01 x_0^1$                    | 9. $10 c x_0^2 a/P$ |
| 2. $B b^2/10^6 a$                  | 10. $10^6/x_0^{13}$ |
| 3. $b^3 x_0 K/a c^{0.68} 10^2$     | 11. $10^2 m/L$      |
| 4. $N/x_0^{13}$                    | 12. $10^2 c/M$      |
| 5. $B/10^2 a$                      | 13. $0.01 T_M'(0)$  |
| 6. $4 y 10^2/a c^4 x_0$            | 14. $0.01 x_0^1$    |
| 7. $0.01 (T_w^{14}/4 \times 10^4)$ | 15. $0.01$          |
| 8. $U/10 a x_0^2 c^{1.88}$         |                     |

Figure C-1

### SYMBOLS FOR COMPUTER ELEMENTS

THE FOLLOWING SYMBOLS ARE USED TO DENOTE THE EQUIPMENT USED

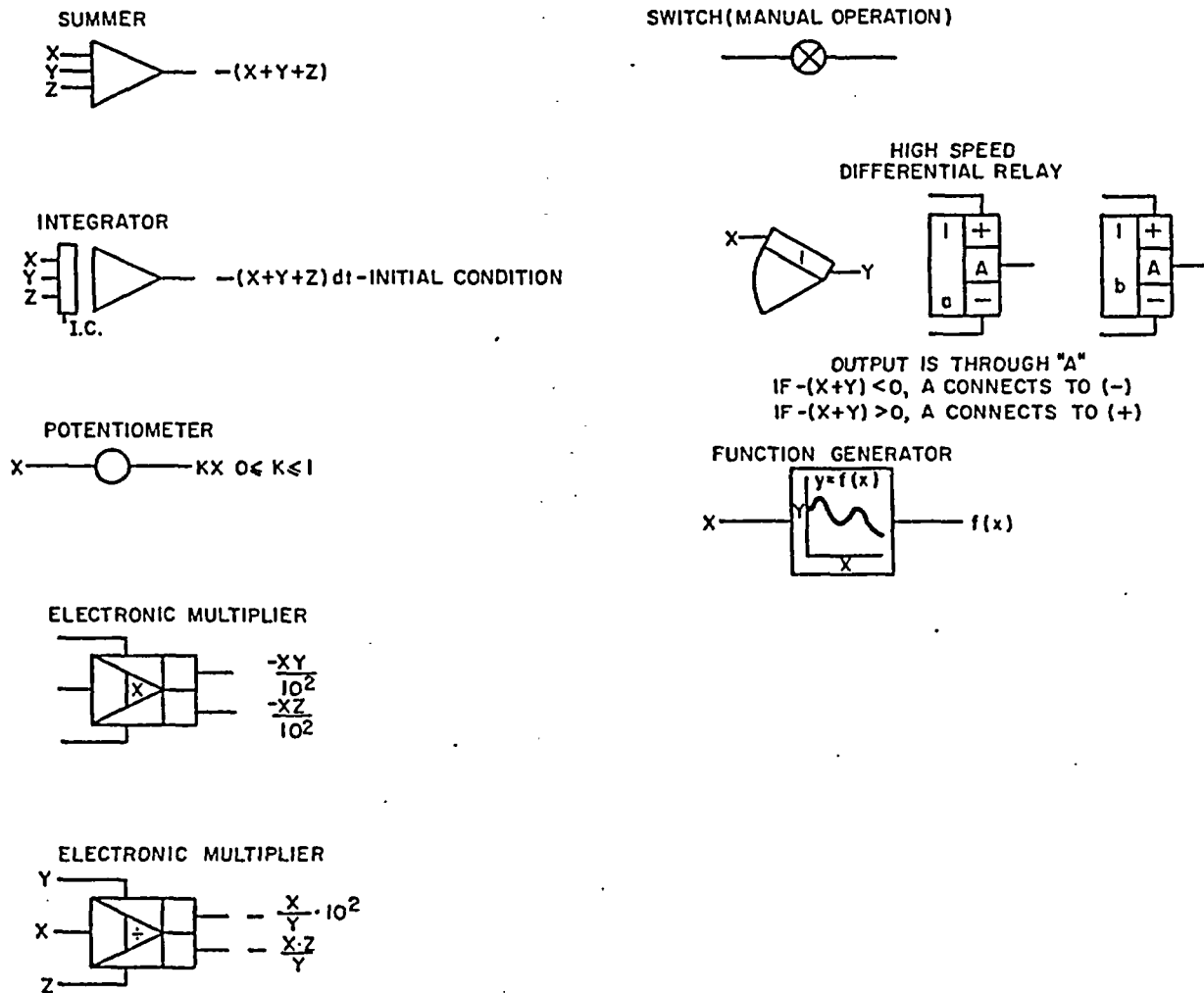


Figure C-2  
CIRCUITS FOR SOLUTION OF EQUATIONS

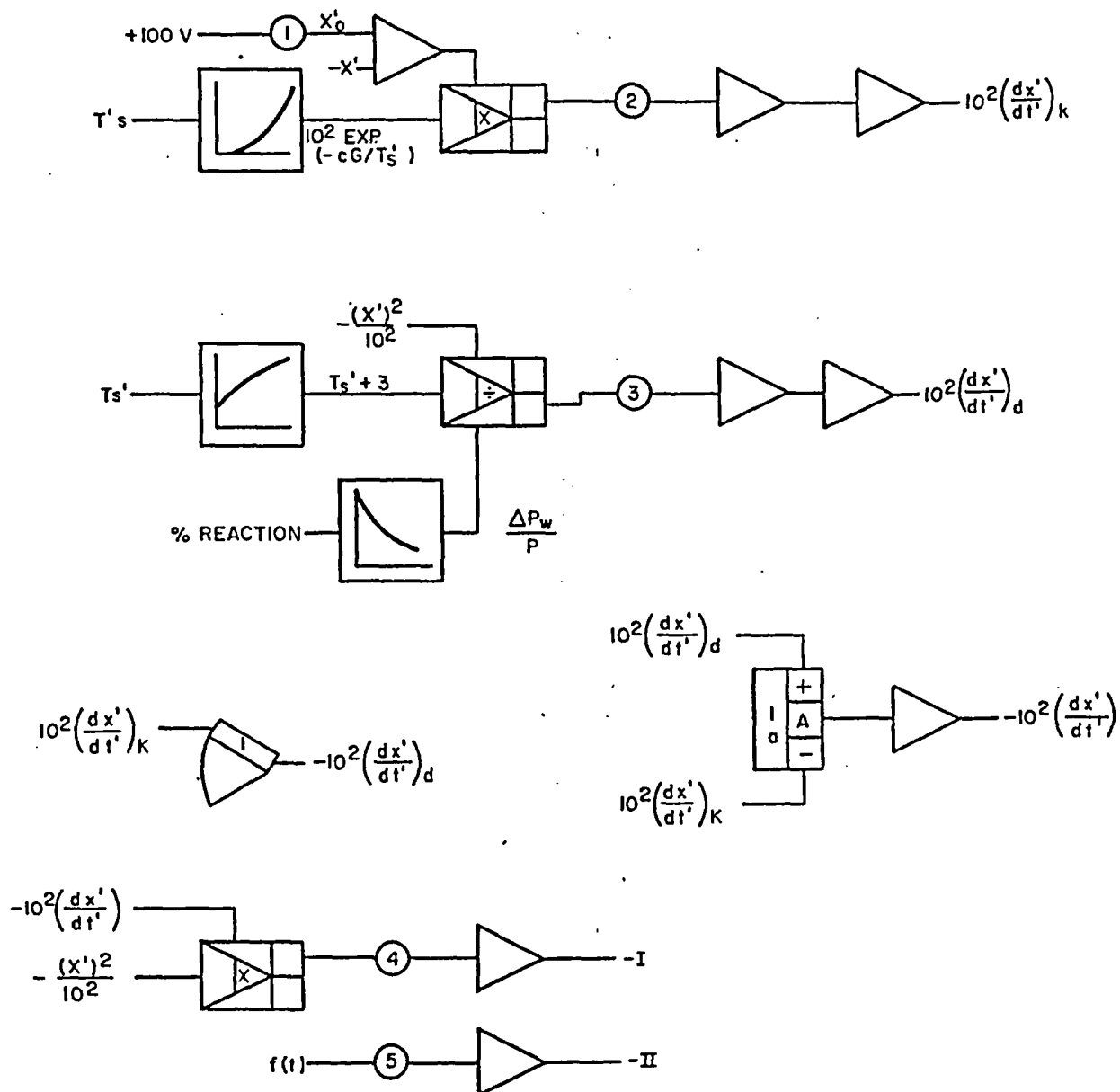


Figure C-3  
CIRCUITS FOR SOLUTION OF EQUATIONS

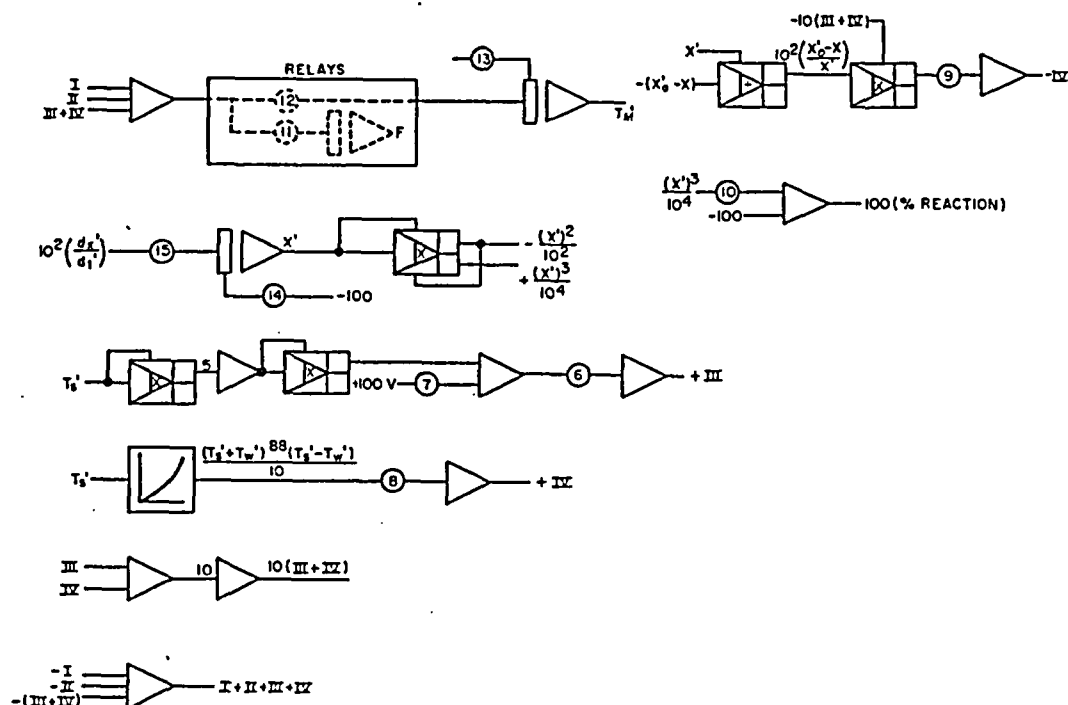
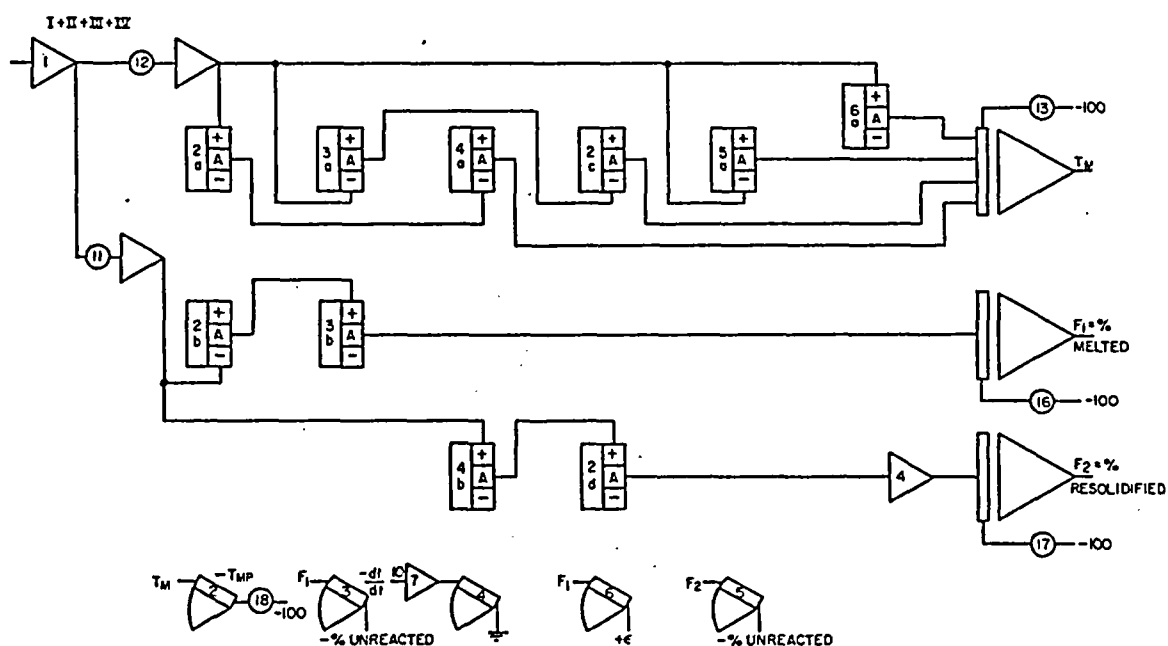


Figure C-4  
CIRCUIT FOR CONTROL DURING PHASE CHANGE



IF  $dt/dt > 0$  AND  $T_M < T_{MP}$ , POT 16 AND 17 = 0  
 IF  $dt/dt < 0$  AND  $T_M < T_{MP}$ , POT 16 = 0, POT 17 = 1.00  
 IF  $T_M > T_{MP}$ , POT 16 = 1.0, POT 17 = 0.0  
 IF  $T_M = T_{MP}$  { AND  $dt/dt > 0$ , SET POT 16 FOR % MELTED AT 1 = 0, POT 17 = 0.0  
 { AND  $dt/dt < 0$ , POT 16 = 0.0 SET POT 17 FOR % SOLID

## Appendix D

ANALYSIS OF THE RATE DATA REPORTED BY  
BOSTROM<sup>(4)</sup> AND LEMMON<sup>(14)</sup>

Studies of the rates of the isothermal reaction of Zircaloy with water and steam were reported by Bostrom (water) and by Lemmon (steam). Lemmon concluded that the results of both studies were best explained in terms of the parabolic rate law, although individual runs showed considerable deviation from the parabolic law slope on log-log plots of the data. It seemed likely that much of this deviation was due to a spuriously slow initial reaction. This might have been due to a limitation caused by gaseous diffusion or to a time lag in bringing the specimen to the temperature of the run. A method of plotting such data is suggested which yields the parabolic rate constant in spite of an initial slow step in the reaction.

The square of the quantity of reaction is plotted as a function of time. The quantity of reaction was determined by collecting the hydrogen generated and is therefore not subject to cumulative errors. The effective time corresponding to the beginning of the run, however, may be uncertain because of the postulated delays in reaching the full reaction rate. One can ignore the first few data points on a plot of this kind, whereas the entire data plot is distorted when plotted on a log-log scale with an uncertainty in zero time.

Individual data points were taken from the published reports and re-plotted in Figures D1 through D4. Lemmon's data at 1400 and 1690 C, Figure D-2, and Bostrom's data at 1750 C, Figure D-4, indicate a delay in reaching the full reaction rate. If the first few points are disregarded, all of the runs are described accurately by a straight line, indicating the validity of the parabolic rate law. There is some indication of a breakaway reaction beyond 300 mg/sq cm reaction in Bostrom's data (90,000 units on the squared plot, Figure D3). This corresponds to an oxide layer thickness of about 500  $\mu$  (20 mils), which is considerably greater oxidation than was achieved in the condenser discharge studies.

The slopes obtained from the data plots are summarized in Table D1. The results are plotted as a function of reciprocal absolute temperature in Figure 16.

Figure D-1  
REACTION BETWEEN ZIRCALOY-2  
AND STEAM  
(Data from Lemmon, Ref. 14)

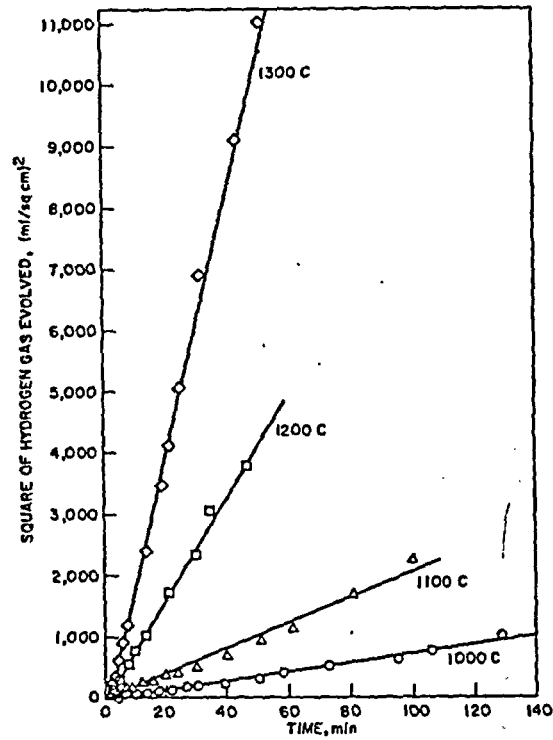


Figure D-2  
REACTION BETWEEN ZIRCALOY-2  
AND STEAM  
(Data from Lemmon, Ref. 14)

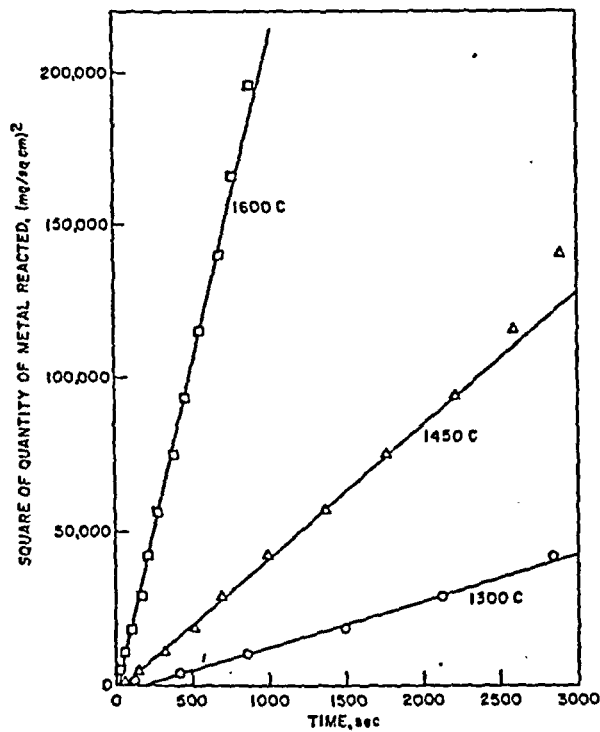
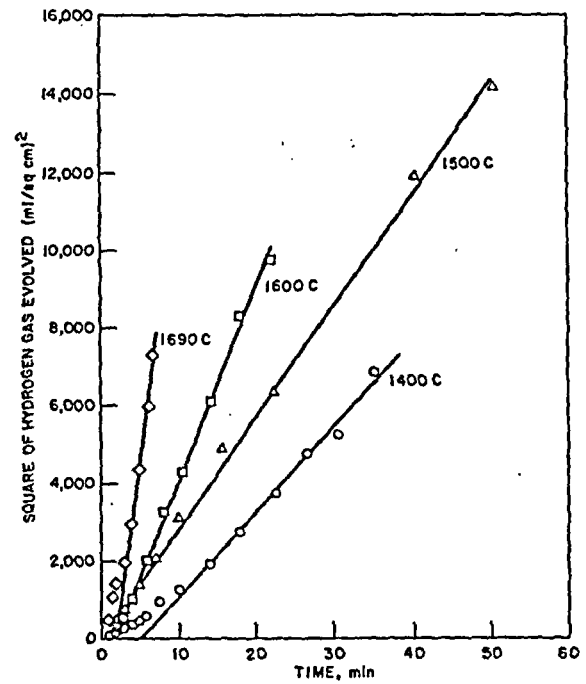


Figure D-3  
REACTION BETWEEN ZIRCALOY-2 AND WATER  
(Data from Bostrom, Ref. 4)



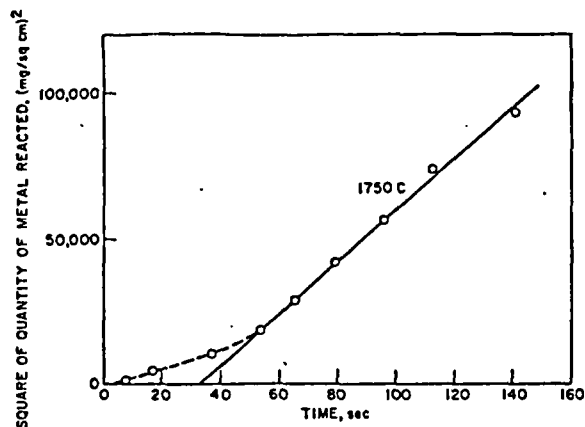


Figure D-4  
REACTION BETWEEN ZIRCALOY-2 AND WATER  
(Data from Bostrom, Ref. 4)

Table D-1

PARABOLIC RATE CONSTANTS RECALCULATED FROM  
THE DATA OF BOSTROM<sup>(4)</sup> AND LEMMON<sup>(14)</sup>

Temperature, C	Parabolic Rate Constants	
	(ml H <sub>2</sub> /sq cm) <sup>2</sup> /min	(mg Zr/sq cm) <sup>2</sup> /sec
Reference 14		
1000	7.45	0.515
1100	20.5	1.42
1200	83.0	5.74
1300	218	15.1
1400	219	15.1
1500	284	19.6
1600	502	34.7
1690	1420	98.1
Reference 4		
1300		15.2
1450		43.6
1600		219
1750		896